DEVELOPMENT OF SENSOR SYSTEMS FOR FOOD QUALITY MONITORING

A Thesis Submitted to
the Graduate School of Engineering and Sciences of
İzmir Institute of Technology
in Partial Fulfillment of the Requirements for the Degree of

DOCTOR OF PHILOSOPHY

in Food Engineering

by
Duygu BÜYÜKTAŞ

December 2022
İZMİR

ACKNOWLEDGEMENTS

The experimental part of this study was accomplished in the packaging laboratory in the Department of Food, Environmental, and Nutritional Sciences at the University of Milan. During this period, I was funded by the Scientific and Technological Research Council of Turkey (TÜBİTAK) under the grant of 2214-A.

Firstly, I would like to thank my supervisor Prof. Dr. Figen KOREL, for her great support, guidance, and encouragement at all times throughout my doctoral study. I would like to express my deepest gratitude to my co-supervisor, Prof. Dr. Stefano FARRIS, for his endless support, concern, and suggestions during this research. This would not be possible without his support. I would like to express my sincere gratitude to my thesis monitoring committee members Prof. Dr. Serdar ÖZÇELİK and Assoc. Prof. Dr. Efe SEZGİN for their valuable contributions and comments throughout thesis monitoring processes. In addition, I am grateful to thesis examining committee members Prof. Dr. Kamile Nazan TURHAN and Assoc. Prof. Dr. Özlem ESMER for their valuable contributions.

During my stay in Milan, many people helped me out with their support and friendship. Especially, I would like to thank Dr. Masoud GHAANI not only for his guidance and patience in the laboratory but also for his friendship. In addition, I am grateful to my dear friends, Daniele CARULLO Begüm AKGÜN, Valeria FRIGERIO, Luana AMOROSO, and Cesare ROVERA for the amazing moments we shared. I am thankful to all my friends I have met at Iztech, but especially to Gözde Seval SÖZBİLEN, Derya BOYACI, and Oğuz UNCU for making this journey bearable.

This thesis was accomplished as a result of great encouragement from each of my family members. I want to express my most sincere thanks to my parents, Hatice BÜYÜKTAŞ, Cevat BÜYÜKTAŞ and my dear sister, Aylin BÜYÜKTAŞ for their endless support and unconditional love.

ABSTRACT

DEVELOPMENT OF SENSOR SYSTEMS FOR FOOD QUALITY MONITORING

The main objective of this thesis is to fabricate electrochemical sensors for the detection of 2,4-diaminotoluene (2,4 TDA), 2,6-diaminotoluene (2,6 TDA), and 4,4´-methylene diphenyl diamine (MDA), possibly carcinogenic primary aromatic amines (PAAs) that poses a serious health risk because they can transfer from multilayer food packages including adhesives based on aromatic polyurethane (PU) systems, to the food. The thesis is based on the following three chapters: (1) Development of a nano-modified glassy carbon electrode for the determination of 2,6-diaminotoluene (2) A screen-printed electrode modified with gold nanoparticles/cellulose nanocrystals for electrochemical detection of 4,4´-methylene diphenyl diamine (3) Development of a nano-modified screen-printed electrode for the determination of 2,4-diaminotoluene.

In this work, full electrochemical characterization of the nano-modified electrodes was carried out, and the electrochemical properties were described. Migration tests were also conducted to modified sensors in order to investigate their potential application in real food systems. The results of this work clearly showed that modified electrochemical sensors allow reliable quantification of the most important primary aromatic amines migrating from packaging materials to food and can be used as an alternative to the commonly used conventional analytical techniques for the detection of these toxic compounds.

ÖZET

GIDA KALİTE TAKİBİ İÇİN SENSÖR SİSTEMLERİ GELİŞTİRİLMESİ

Bu tezin başlıca amacı, çok katmanlı ambalaj malzemelerinden gıdaya geçiş yapan insan sağlığına zararlı kanserojen primer aromatik aminlerin hızlı tespiti için nanomalzemeler ile modifiye edilerek seçiciliği arttırılmış elektrokimyasal sensörlerin üretilmesi ve gerçek gıda sistemlerinde potansiyel kullanımlarının araştırılmasıdır. Bu tez çalışması temelde üç bölümden oluşmakta olup bunlar şu şekilde sıralanmaktadır: (1) 2,6-diaminotoluenin tayini için nano-modifiye camsı karbon electrotun geliştirilmesi (2) 4,4'-metilen difenil diaminin elektrokimyasal tespiti için altın nanopartiküller/selüloz nanokristaller ile modifiye edilmiş ekran baskılı bir elektrot geliştirilmesi (3) 2,4-diaminotoluenin tayini için nano-modifiye ekran baskılı bir electrot geliştirilmesi.

Bu çalışmada, farklı nanomalzemelerle modifiye edilmiş camsı karbon elektrot ile ekran baskılı elektrotların tüm elektrokimyasal karakterizasyonu yapılmıştır. Ayrıca, bu elektrotların gerçek ambalaj sistemlerindeki potansiyel kullanımlarının tespit edilmesi için migrasyon testleri uygulanmıştır. Bu tez çalışması, geliştirilen nano-modifiye sensörlerin çok katmanlı ambalaj malzemesinden gıdaya geçiş yapması olası primer aromatik aminlerin seçici olarak tespitinde kullanılabileceğini, ve bu maddelerin tespitinde yaygın olarak kullanılan konvensiyonel analitik yöntemlere alternatif olabileceğini göstermiştir.

TABLE OF CONTENTS

LIST OF FIGURES

Figure **Page**

Figure **Page**

Figure **Page**

LIST OF TABLES

Table **Page**

CHAPTER 1

INTRODUCTION

Multilayer materials represent the first-choice option for many different food applications because they allow to achieve an outstanding overall performance by combining the properties of each individual, such as printability, barrier properties against gases and vapors, mechanical performance, and thermal properties (e.g., sealability) (Goulas, Riganakos, and Kontominas 2003). Multilayer materials are manufactured by the converting industry, which deals with processing operations (such as printing, coating, and laminating) to convert the pristine flat web into an intermediate form or the final packaging material. Among the wide variety of adhesives, polyurethane (PU) adhesives are the most extensively used by the converting industry owing to their unrivaled performance, as demonstrated by their largest market share in food-contact adhesives (Yan et al. 2020). However, a risk associated with PU adhesives is the possible formation of undesired by-products, also defined as non-intentionally added substances (NIAS), such as cyclic polyesters oligomers primary aromatic amines (PAAs) (Ubeda et al. 2020). The origin of PAAs, while primarily linked to residual (unreacted) isocyanic monomers, has more recently been ascribed to the cleavage of secondary bonds on the main PU backbone (e.g., biuret and especially allophanate bonds) due to thermal stresses, such as those represented by conventional thermal operations (e.g., pasteurization and sterilization) and cooking methods (e.g., vacuum-cooking, microwaving, etc.) (Campanella et al. 2015). In spite of the large number of PAAs, those of relevance for the food packaging sector are the 4, 4'-methylene diphenyl diamine, the 2,6-diaminotoluene (2,6-TDA), and the 2,4-diaminotoluene (2,4-TDA), which arise from the methylene diphenyl diisocyanate (MDI) and toluene diisocyanate (TDI) isocyanic monomers. These monomers account for almost the totality of isocyanic monomers used for the obtainment of aromatic PU adhesive systems. TDI monomers, in particular, find predominant use in the manufacturing of solvent-based OH-terminated PU adhesives. In this case, a mixture of the two isomers (2,6-toluene diisocyanate and 2,4-toluene diisocyanate) is most often used.

Possible contamination of food by PAAs poses a serious threat to the consumers' health because PAAs have been defined as "possibly carcinogenic to humans" (Vineis and Pirastu 1997). The use of aromatic-based PU adhesives has been forbidden by FDA in the U.S. According to European Regulation 10/2011, plastic material and articles shall not release PAAs in detectable quantity in food or food simulants. The limit is set to 0.01 mg of substances per kg of food or food simulant (European Commission 2011; Sanchis, Yusa, and Coscolla 2017; Mortensen et al. 2005). Turkish Food Codex plastic in contact with food substances and materials communique No. 2019/44, were updated to align with EU plastic regulation No. 10/2011 (European Commission 2011; Turkish Food Codex 2019). From a practical point of view, the detection of PAAs occurs mainly using the spectrophotometric method developed by the German Federal Institute for Health Protection of Consumers and Veterinary Medicine (BgVV) (Brauer and Funke 1991). According to this method, the quantification of PAAs is expressed as equivalent to aniline. The main drawback associated with this method is its non-selectivity, which may lead to overestimate the ultimate quantification of PAAs in food simulants (Aznar, Canellas, and Nerin 2009; Brede and Skjevrak 2004). For achieving a selective detection of PAAs, other analytical techniques have been proposed as alternatives to the spectrophotometric method. Among others, chromatography (Cai et al. 2020), mass spectrometry (Sanchis, Coscolla, and Yusa 2019), capillary electrophoresis (Mattarozzi et al., 2013), and electrochemical methods (Chen et al. 2015) proved to be effective for the detection of trace amounts of PAAs transferred from the packaging material. However, also the above methods have drawbacks. For example, they are complex and time-consuming especially as far as the sample preparation is concerned. In addition, the high cost of the necessary equipment, together with the necessity of specialized operators, makes these methods unaffordable for most players in the converting industry (Ghaani et al. 2018a; Ghaani et al. 2018b). For these reasons, new analytical tools that are selective, sensitive, easy to use, and inexpensive for the determination of PAAs may represent an important advancement in the food industry, especially for quality control purposes (Ghaani et al. 2018a; Viswanathan and Radecki 2008).

In recent years, electrochemical methods have attracted much attention as reliable analytical devices because they proved to possess all the aforementioned attributes. However, electrochemical sensors do not always exhibit adequate performance, especially in terms of selectivity, due to the similar chemical structures of PAAs (Chen et al. 2015). To improve the electrode's overall performance, the surface of the electrode

can be modified using nanoparticles, such as carbon-based nanomaterials and metallic nanoparticles (Rassaei et al. 2011; Wang et al. 2014; Wang et al. 2015; Zhang, Sun, and Cao 2020). These nanosized entities help, for example, prevent fouling and increase the selectivity and electrocatalytic properties of the sensor owing to the large surface area and high electrical conductivity (Hanssen, Siraj, and Wong 2016).

In light of the above-mentioned knowledge, this doctoral thesis study is designated to comprise of the following three chapters:

In Chapter 3, it was aimed to develop an electrochemical sensor for the detection and quantification of 2,6-TDA, which is one of the primary aromatic amines migrating from packaging material into food. For this purpose, the electrochemical sensor was modified with multi-walled carbon nanotubes (MWCNTs) and carbon mesoporous (MCNs) to increase the selectivity of the electrode against the target analyte.

In Chapter 4, it was aimed to fabricate a screen-printed electrode to quantify 4,4'-methylene diphenyl diamine as a rapid, selective, sensitive, and reliable analytical tool. Gold nanoparticles (AuNPs) and cellulose nanocrystals (CNCs), which are promising hybrid materials with unique properties, were used in the modification of the electrode.

Lastly, in Chapter 5, a screen-printed electrode, modified with AuNPs-CNCs, was developed for the detection of 2,4-diaminotoluene (2,4-TDA), which is one of the most important primary aromatic amines that can transfer from packaging and contaminate food.

In all three chapters, a detailed electrochemical characterization of each modified electrode was investigated, and their capabilities to be used in real samples were evaluated by a migration test.

CHAPTER 2

LITERATURE REVIEW

2.1. Multilayer packaging

Multilayer packaging is a novel technique that combines the distinct functionalities of numerous polymers to obtain a package with superior performance concerning improved protection and durability. Food packaging materials must satisfy specific requirements such as protection/preservation, machinability, promotion, and convenience. In addition, they should provide cost-effectiveness and abide by all aspects of food safety (Kaiser, Schmid, and Schlummer 2017). In most cases, however, a single monolayer of polymer cannot fulfill all these criteria. Thus, the motivation for manufacturing multilayer packaging is to create a single packing structure with multiple functional properties that meet all the sophisticated requirements of packaging. Multilayer packaging as a whole unites each layer's benefits regarding improved barrier properties, mechanical integrity, and functional properties (Anukiruthika et al. 2020). Even though multilayer packaging materials typically consist of three to twelve layers, when it comes to food packaging, they contain at most seven layers (Butler and Morris 2016) (Figure 2.1).

Multilayer films with improved stability, strength, appearance and functional qualities can be manufactured using the lamination technique. A web-typed structure can be created by laminating a variety of polymeric and nonpolymeric materials, one on top of the other until they posses the appropriate qualities. There are numerous ways to make laminates, including extrusion, adhesive, wax, and hot melt lamination (Wagner 2016). In converting lines, lamination mediated by adhesives is favored over other methods due to its low cost and ease of production (Rosato 1998).

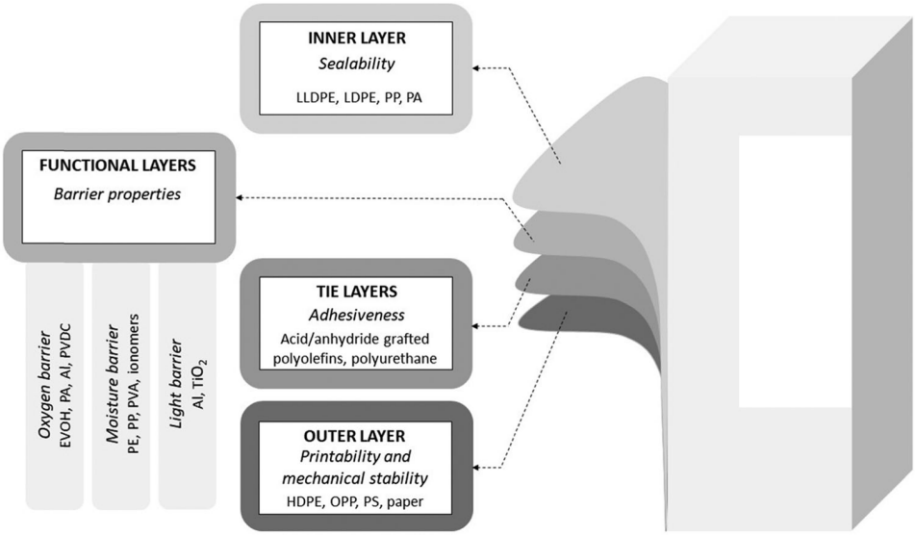

Figure 2.1. Layers of multilayer packaging (Source: Dixon 2011; Morris 2016).

In order to promote adhesion and strengthen layer bonding, adhesive or tie layers are frequently placed between two different polymeric materials. Among the many adhesive systems on the market, polyurethane (PU) adhesives are well-known for their superior flexibility, mechanical and adhesion properties, and weathering resistance (Malucelli et al. 2005).

PU adhesives are typically derived from reactive systems that typically contain two main components, one with NCO-terminated isocyanic moieties and the other with OH-terminated hydroxyl groups. When these components are combined, chemical reactions (i.e., chain extension) occur, which bind the applied materials into a solid layer of high molecular weight PU adhesive. After lamination, the adhesive components react, increasing the molecular weight of the PU adhesive to achieve the required performance (Meier-Westhues 2007). Because the adhesives are made of reactive chemicals that are expected to polymerize by linear extension and/or cross-linking, government food safety-related agencies - the Food and Drug Administration (FDA) in the United States and the European Food Safety Authority (EFSA) - have established a strict legislative body to control the risk associated with the potential migration of toxic substances from the adhesives to the food, which in turn can cause adverse health effects in humans (de Fatima Poças and Hogg 2007).

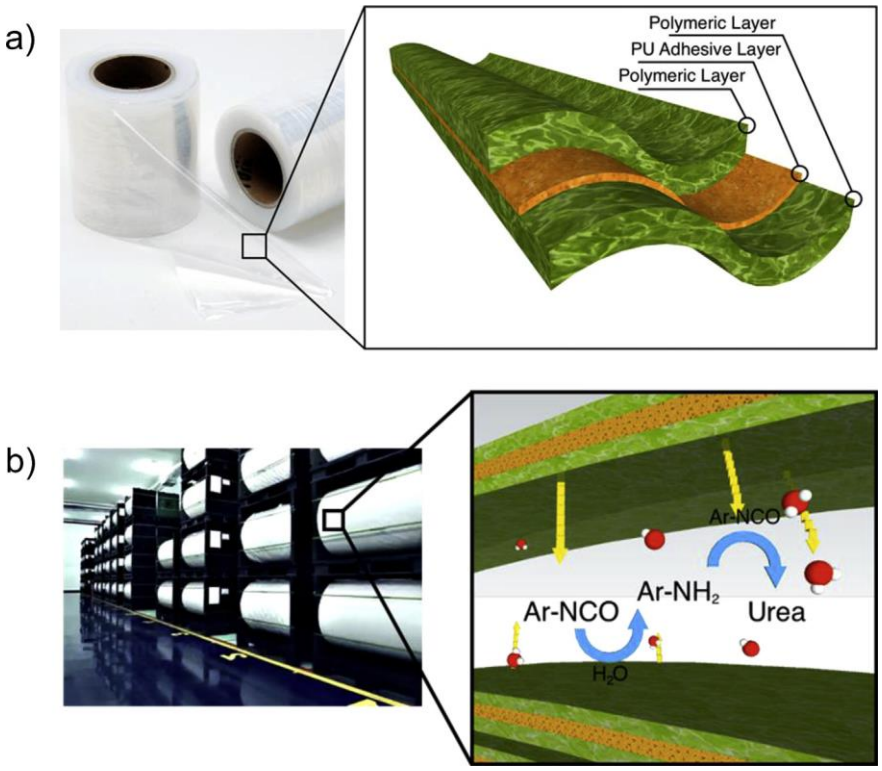

Figure 2.2. (a) Schematic representation of a PU adhesive-based laminate packaging material (3-layer structure). (b) Formation of poly(urea) in PU adhesive-based multilayer packaging materials wound in reels. (red-white spheres: water molecules; Ar-NCO: aromatic isocyanate monomers; Ar-NH_2: aromatic amines) (Source: Campanella et al. 2015).

In the case of multilayer packaging materials, such as pouches, trays, bags, wrappers, etc., the probable presence of primary aromatic amines (PAAs) in the food matrix is one of the principal concerns associated with PU adhesive systems (Ellendt, Gutsche, and Steiner 2003). According to the International Agency for Research on Cancer, the possible risk associated with PAAs stems from the suspected carcinogenic activity of, most notably, 2,4 and 2,6-diaminotoluene and 4,4-methylene diphenyl diamine, which can have an adverse impact on human health (Vineis and Pirastu 1997; Campanella et al. 2015).

2.2. Formation of primary aromatic amines

Primary aromatic amines (PAAs) are a broad class of organic compounds in which basic configurations consist of an aromatic ring with an amine group, aniline, to a complex set of rings with multiple amines. There are two major formation pathways of PAAs. They are mainly derived from residual (unreacted) isocyanic monomers arising from incomplete curing of the main polyurethane adhesive (Brede, Skjevrak, and Herikstad 2003). Within the particular time frame, that is, immediately after the lamination process and prior to the packaging operations, the isocyanic monomers have a possibility of coming into contact with the air (and consequently, contact with the surrounding environmental moisture) in the space between two adjacent coils of the laminated material that is wound in a reel. The reaction between the remaining isocyanic monomer and water molecules causes the formation of primary aromatic amines (Campanella et al., 2015). In practice, this issue is addressed by storing the laminate reels for the time needed to consume the free isocyanic monomer by either reacting with the main adhesive system or reacting, after migration, with the water molecules of the environmental humidity, always present in traces between the laminate coils (European Commission 2006).

However, this approach only takes into account the potential risk related to unreacted isocyanic monomers due to the insufficient curing process. It neglects the neo-formed PAAs that could result from the post-heat treatments of packaged foods that are generally applied to preserve food products (Lee, Yam and Piergiovanni 2008). Some secondary bonds displaced on the main PU backbone, such as allophanate and biuret bonds, may be disrupted by these heat treatments. Following the addition reactions of isocyanic monomers and urethane and ureic groups, allophanate and biuret are produced. Furthermore, the polymerization temperature may influence the formation of allophanate and biuret bonds, as higher temperatures promote the formation of allophanate and biuret linkages (Lapprand et al. 2005). The allophanate bonds on the primary PU adhesive backbone exceed the biuret bonds owing to the greater number of urethane groups than ureic groups. Moreover, allophanate bonds derived from aromatic isocyanic monomers are thermally less stable when compared to those acquired from aliphatic isocyanic monomers. As a result, the low thermal stability of allophanates and, to a lesser extent, biurets can be identified as the primary source of reproduction of isocyanic monomers in

laminate structures fabricated with aromatic polyurethane adhesive systems. Allophanate and biuret bonds start to break down at about 70 °C and the rate at which the monomer is reformed increases as tempreature increases, until it can be considered complete for temperatures above 105 °C (Yoshitake and Furukawa 1995). Consequently, there will always be the reformation of isocyanic monomers due to the cleavage of allophanate linkage caused by thermal energy input in the case multilayer packaging produced using PU adhesives is subjected to thermal treatment for preservative purposes (Figure 2.3a).

Since the internal moisture of the package facilitates the transfer of newly created PAAs from the inner surface of the package, the migration of isocyanic monomers will continue in case they are used for PAAs synthesis. That is to say, the internal moisture stimulates the formation of PAAs, which then migrate from the inner packaging layer to the food matrix (Ghaani et al. 2018a) (Figure 2.3b).

Because of the risk associated with PAAs (carcinogenic substances), it becomes clear the importance of investigating the formation, migration, and mechanisms of control of PAAs from food packaging materials comprehensively. In this regard, recently, various analytical techniques (mainly spectrophotometric/colorimetric and chromatographic methods) have been conducted for the detection of PAAs migrating from packaging materials, including PU adhesives, into food. However, all these conventional techniques have some disadvantages. For instance, they are complicated and time-consuming, especially when the sample preparation is concerned. Additionally, the high cost of the necessary equipment, besides the necessity of specialized operators, makes these methods unaffordable for most players in the converting industry (Brede, Skjevrak, and Herikstad 2004; Mattarozzi et al. 2013; Wang and Chen 2009; Chen et al. 2015; Ghaani et al. 2018b).

Especially because of legal obligations, companies dealing with food packaging, both manufacturers and converters, are increasingly looking for new devices and analytical tools to enable the determination of hazardous substances that can migrate from the packaging material to the food. However, due to the aforementioned disadvantages of the common analytical methods, packaging companies most often prefer to outsource the food contact material procedures in their production. Electrochemical sensors, because of sensitivity, selectivity, lower cost, and ease of use compared to conventional analytical instrumentation, probably represent the most promising solution for the years to come. For this scope, researchers worked to develop new electrochemical sensors for detecting

hazardous analytes in food packaging materials (Khanna et al. 2018; Fu et al. 2016; Long et al. 2015).

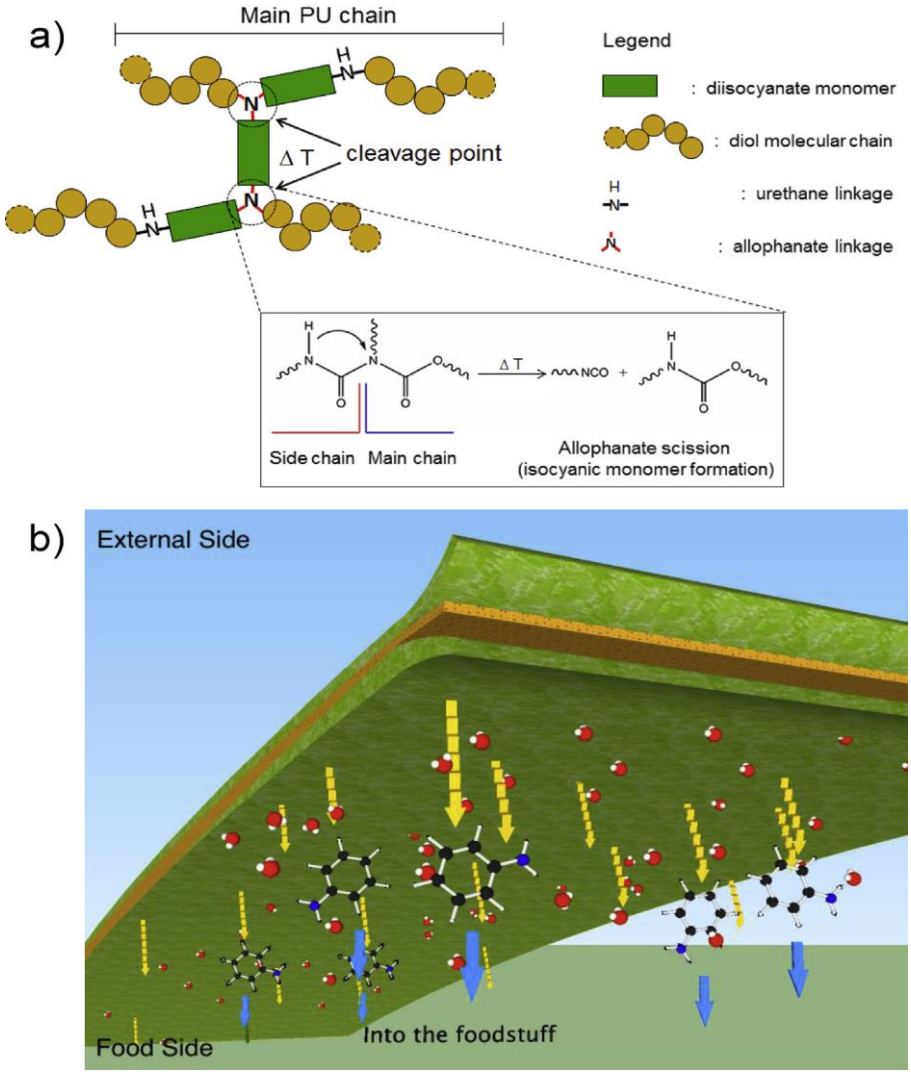

Figure 2.3. (a) Formation of the isocyanic monomer from the thermal cleavage of the allophanate linkage (b) Potential migration of PAAs from the packaging to the food matrix (red-white spheres: water molecules; black-blue spheres: representative aromatic amine; yellow arrows: migration of the isocyanic monomer; cyan arrows: washing-out effect of environmental moisture) (Source: Campanella et al. 2015).

2.3. Electrochemical sensors

Electrochemistry is the study of the interactions between electrical and chemical effects. A significant part of this field is concerned with the investigation of chemical changes caused by the passage of an electric current as well as the generation of electrical energy through chemical reactions (Bard, Faulkner, and White 2022).

Electrochemical sensors are a significant subclass of chemical sensors that operate on electrochemical principles. The transducer is the electrode in this type of sensor (Wang 2001). A typical electrochemical sensor is made up of three main electrodes: sensing (working electrode), counter, and reference electrodes, all of which are interconnected to a potentiostat device. Electrochemical sensors operate on the basis of redox reactions that occur at the electrode/analyte interface when a voltage is applied via a potentiostat. The transfer of electrons between electrodes and electroactive species produces a current that is proportional to the analyte concentration. The potentiostat is connected directly to a display unit, which is generally a computer. This computer is used to display the variations in current and voltage during the experiment and to control the device using specialized software and a unique electrochemical method (Ghaani et al. 2016; Bard, Faulkner, and White 2022; Rassaei et al. 2011). Figure 2.4 depicts an overall view of an electrochemical sensor.

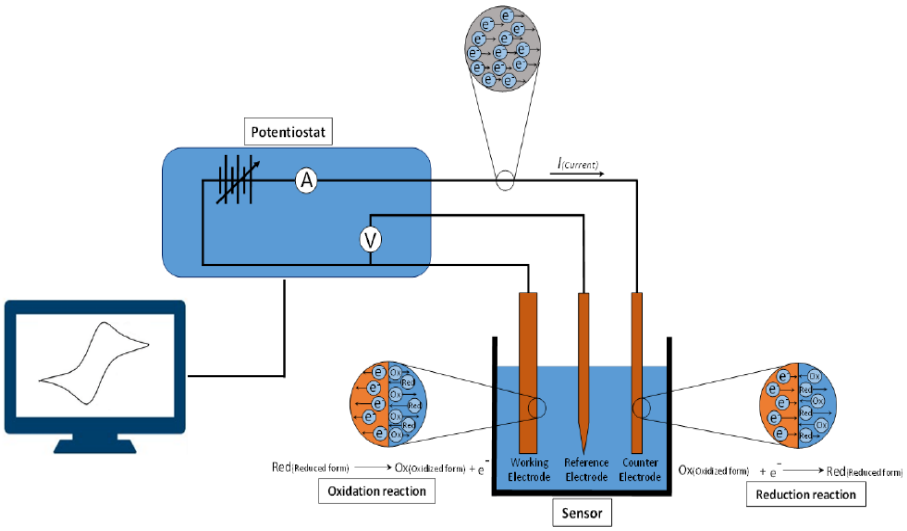

Figure 2.4. Shematic representation of an electrochemical sensor system (Source: Ghaani, 2018)

A reference electrode is an electrode that has a constant and defined potential. Fundamental characteristics of a proper reference electrode are a stable potential and chemical reaction, a well-known half reaction, ease of manufacture, and the ability to monitor the analyte without interfering. The silver–silver chloride (Ag-AgCl) electrode and the saturated calomel (Hg_2Cl_2) electrode are the most commonly used as reference electrodes in electrochemical measurements (Bard, Inzelt, and Scholz 2012).

A current flows through the working electrode and the counter electrode in an electrolysis cell, which includes all 2- and 3-electrode cells. Most counter electrodes are made of a conducting and inert substance, such as graphite or noble metals like platinum (Bard, Inzelt, and Scholz 2012).

A working electrode monitors the redox reaction that occurs at the working electrode/analyte interface after the potentiostat applies a voltage. The transfer of electrons between electrodes and electroactive species produces a current proportional to the analyte concentration. A variety of working electrodes, including mercury, glassy carbon, carbon paste, platinum, and gold electrodes can be used in electrochemical measurements (Ghaani et al. 2016).

Different chemical and physical modifications have been proposed in recent years to improve the analytical performance of the electrode to overcome the limited selectivity and sensitivity of bare working electrodes. Sensitivity allows characterization of the analytical performance of the sensor while making it possible to define its detection limit, a measure of the smallest concentration that can be determined with a specified precision or reproducibility, described as the signal-to-noise ratio (S/N). Improving the sensitivity of electrochemical sensors is a goal for many different applications to detect the smaller amounts of the target analyte. Among different strategies, modifying the electrode surface with nano-sized entities, such as carbon nanotubes, gold nanoparticles, iron oxide, graphene, etc., is one of the most common approaches for increasing the sensitivity of the sensors (Hanssen, Siraj, and Wong 2016).

2.3.1. Electrochemical sensors in the food industry

In the food industry, the development of electrochemical sensors has frequently been designed at resolving some of the major drawbacks associated with conventional spectrometric and chromatographic techniques. While these approaches provide high

sensitivity and selectivity, they are expensive, time-consuming, require difficult sample preparation, and require specialized personnel. Spectrometric and chromatographic techniques are rarely used for on-line food quality control (Wang et al. 2018; Ghaani et al. 2018a).

In reality, the food industry requires analytical devices that can fulfill the requirements such as being simple to operate, real-time, no hygiene risk, sensitive, physically robust and stable, and non-destructive.

In addition, recent advancements in material chemistry and physics, as well as the field of information processing, have led to the development of sensors for the detection of multiple analytes. Some examples of electrochemical sensors in different food groups are displayed in Tables 2.1-2.4.

Table 2.1. Some applications of electrochemical sensors in Meat products

Modifier	**Analyte**	**Linear range**	**Limit of detection**	**Reference**
Iron(II) Phthalocyanine, Gold nanoparticles	Nitrite	2-120 μM	0.35 μM	Dorovskikh et al. 2022
Reduced graphene oxide, gold nanoparticles, polyvinyl alcohol	*E.coli* O157:H7	9.2 - 9.2×10^{8} CFU/mL	9.34 CFU/mL	Qaanei, Taheri and Eskandari 2021
Carboxylated single-walled carbon nanotubes, Chitosan	Cephalexin	1- 800 ng/ml	45.7 ng/ml	Yu et al. 2020
Gold nanoparticles, carboxylic group-functionalized single-walled carbon nanotubes, chitosan	T-2 toxin	0.01-100 μg/L	0.13 μg/L	Wang et al. 2018

Cont. on the next page

Table 2.1. (cont.)

Au, Reduced graphene oxide, Poly(diallyldimethylammonium chloride)	Nitrite	0.5×10^{-6} 8.5×10^{-6} M	0.04×10^{-6} M	Jiao et al., 2015

Table 2.2. Some applications of electrochemical sensors in Fish products

Modifier	**Analyte**	**Linear range**	**Limit of detection**	**Reference**
$ZnIn_2S_4$/UiO-66-NH_2	Xanthine Hypoxanthine	0.025-40μM 0.3-40 μM	0.0083 μM 0.1 μM	Song et al. 2022
Gold nanoparticles, Manganese dioxide	Histamine	0.3-5.1 μM	0.08 μM	Knezevic et al. 2020
Multiwalled carbon nanotubes, Silver-argentous oxide nanoparticles	Histamine	5-200 mg/L	0.18 μM	Butwong et al. 2019
Reduced graphene oxide	Octapamine Tyramine	0.5-40 μM 0.1-25 μM	0.1 μM 0.03 μM	Zhang, Sun, and Cao 2016
Graphene, Gold nanoparticles	Nitric oxide	36×10^{-9} - 20×10^{-6} M	18×10^{-9} M	Wang et al. 2015
Oligonucleotide, Dendritic gold nanoparticles, Reduced graphene	*Listeria monocytogenes*	1.010^{-12} - 1.0×10^{-6} CFU/mL	2.9×10^{-13} CFU/mL	Sun et al. 2012

Table 2.3. Some applications of electrochemical sensors in Dairy product

Modifier	**Analyte**	**Linear range**	**Limit of detection**	**Reference**
Graphitic carbon nitride, magnetic chitosan	Lactose	0.9-100 mM	0.3 mM	Nasiri et al. 2023
Multi-walled carbon nanotubes	Vanillin	4.15-294.12 μM	3.44 μM	Kouhi et al. 2022
Graphene oxide, Cu-Ag core-shell nanoparticles	Sulfamethazine	10-1000 mM	0.46 mM	Feizollahi et al. 2021
Gold nanoparticles, polypyrrole composite	Formaldehyde	-	0.4 mM	Xi et al. 2020
Reduced graphene oxide, Copper nanoflowers	Melamine	10×10^{-9} - 9.0×10^{-8} M	5.0×10^{-9} M	Daizy et al. 2019
Cadmium doped antimony oxide nanostructures	Melamine	0.05 nM-0.5 mM	$1,4\times10^{-11}$ M	Rahman and Ahmed 2018
Nano iron oxide, Carbon nanotubes	Hydrogen peroxide	1.2×10^{-6} - 21.6×10^{-6} M	3.7×10^{-9} M	Thandavan et al. 2015

Table 2.4. Some applications of electrochemical sensors in Juice products

Modifier	Analyte	Linear range	Limit of detection	Reference
Tungsten disulfide, Gadolinium cobaltite	Quercetin	0.001-329 μM	0.003 μM	Mariyappan et al. 2022
Silver nanoparticles, Multi-walled carbon nanotubes	Cyanide	0.1-210 μM	4 nM	Zhang, Sun, and Cao 2020
Poly(L-arginine), Reduced graphene oxide	Tartrazine	1.00×10^{-6} - 2.50×10^{-4} mol/L	2.5×10^{-7} mol/L	Wang et al. 2020
Graphen oxide, polypyrrole	Phenothrin	2.5×10^{-8} - 2.0×10^{-5} M	13.8×10^{-9} M	Tefera et al. 2018
P-Aminophenol, Multi-walled carbon nanotubes	Vitamin C	2×10^{-7} - 1.2×10^{-7} M	8×10^{-8} M	Gheibi et al. 2015
Zinc oxide, Carbon nanotubes	Ascorbic acid	0.1×10^{-6} - 450×10^{-6} M	0.07×10^{-6} M	Bijad, Karimi-Maleh, and Khalilzadeh 2013

2.3.2. Electrochemical sensors in food packaging

Packaging is an important component in the food manufacturing process. Despite the well-known benefits that packaging provides to consumers, it has been the subject of numerous debates regarding the environmental impact and the health issues related to the use of packaging materials. Due to consumers' growing awareness of the possible risks associated with food contact materials (FCMs), the scientific community and legislative

authorities have taken an interest in assessing the migration of compounds from packaging materials to food. Especially because of legal obligations, companies dealing with food packaging, both manufacturers and converters, are increasingly looking to new devices/analytical tools enabling the determination of hazardous substances that can migrate from the packaging material to the food (Arvanitoyannis and Bosena 2004). Table 2.5 displays studies on electrochemical sensors used to detect compounds that are important in food packaging.

Table 2.5**.** Some applications of electrochemical sensors in Food Packaging

Modifier	**Analyte**	**Linear range**	**Limit of detection**	**Reference**
Graphene oxide, MIP	Bisphenol A	0.006-0.1 μM - 0.2-20 μM	0.003 μM	Dadkhah et al. 2016
MIP, Graphene	Bisphenol A	8.0 nM-1.0 μM 1.0-20 μM	6.0 nM	Deng, Xu, and Kuang 2014
MWCNTs, AuNPs, MIP	Bisphenol A	1.13×10^{-7}-8.21×10^{-3} mol/L	3.6×10^{-9} mol/L	Huang et al. 2011
Graphene oxide, AuNPs, MIP	Dibutyl phthalate	2.5×10^{-9}-5.0×10^{-6} mol/L	2.0×10^{-6} mol/L	Li et al., 2015

CHAPTER 3

DEVELOPMENT OF A NANO-MODIFIED GLASSY CARBON ELECTRODE FOR THE DETERMINATION OF 2,6-DIAMINOTOLUENE (TDA)

Redrafted and modified from:

Büyüktaş, Duygu, Masoud Ghaani, Cesare Rovera, Richard T. Olsson, Figen Korel, and Stefano Farris. "Development of a nano-modified glassy carbon electrode for the determination of 2, 6-diaminotoluene (TDA)." *Food Packaging and Shelf Life* 29 (2021): 100714.

3.1. Introduction

Recently, electrochemical sensors have attracted much attention as a novel analytical tool in the determination of numerous compounds since they are more sensitive, and selective and their response time is faster when compared to conventional analytical techniques (Ghaani et al. 2016; Yu et al. 2018). Their working principle is based on the electrochemical (redox) reaction that occurs on the surface of the working electrode. By virtue of the applied voltage that causes this redox reaction, a measurable current proportional to analyte concentration is obtained. On the other hand, the fouling phenomenon, which can negatively affect the detection limit, sensitivity, and reproducibility, is the most limiting factor while using a bare electrode. Therefore, the use of nanomaterials to modify the bare electrode surface to overcome the aforementioned drawback and enhance electrode performance has been suggested as a promising strategy (Hanssen, Siraj, and Wong 2016; Nasirizadeh et al. 2016). In this regard, carbon-based nanomaterials and metallic nanoparticles can be used to produce nanocomposite surface modifiers due to their electrical conductivity, large surface area, and anti-fouling property (Fakhari et al. 2015; Ghaani et al. 2018a).

In this chapter, we described the development of a novel selective electrochemical sensor modified with carbon nanotubes (MWCNTs) and mesoporous carbon nanoparticles (MCNs) for the quantification of 2,6- diaminotoluene (2,6-TDA), which is a typical PAAs that can transfer from PU adhesives across the packaging thickness, eventually contaminating the food. The modified electrochemical sensor was deeply characterized as far as its electrochemical properties were concerned. The sensor modification that exploited the synergism between MWCNTs and MCNs led to a high selective, high sensitive, and with a lower limit of detection modified MWCNT-MCN/GCE, in addition to the prevention of fouling on the electrode surface. Finally, the analytical behavior of the sensor was assessed simulating a real-case scenario using a typical packaging configuration.

3.2. Experimental Study

In the following sections, both materials and methods performed for the quantification of 2,6-TDA were given in detail.

3.2.1. Materials

2,6-TDA (analytical grade 98 %, molar mass 122.17 g mol^{-1}) and MCNs (500 nm particle size) were bought from Sigma Aldrich (Milan, Italy). Phosphoric acid (85–90%), boric acid (99.999% trace metals basis), and acetic acid (99%) were purchased from Sigma Aldrich (Milan, Italy). Ethylene glycol monomethyl ether (EGMe) was bought from Merck (Milan, Italy), while alumina powder (type DX, 0.05 μm average size) was bought from EMS (Hatfield, PA, U.S.). Britton–Robinson (B–R) universal buffer (0.04 M boric acid, 0.04 M acetic acid and 0.04 M phosphoric acid) was prepared in deionized water and was tested as the supporting electrolyte.

Electrochemical experiments were performed using a PGSTAT 302 N potentiostat (Metrohm, Herisau, Switzerland) equipped with a three-electrode electrochemical cell on which was mounted a modified glassy carbon (working) electrode, a platinum (counter/auxiliary) electrode, and an Ag/AgCl (reference) electrode saturated with 3 M KCl, all immersed in a double-jacket 80 mL glass cell (Bio-Logic, Claix, France). The software Nova 2.0 was used throughout the electrochemical

experiments. The pH measurements were performed with a BASIC 20+ pH meter (Crison Instruments, S.A. Barcelona, Spain). All the experiments were carried out at 25 ± 0.5 ◦C.

3.2.2. Methods

The methods given below were performed to investigate the behavior of 2,6-TDA on glassy carbon electrode surface.

3.2.2.1. Electrode Modification

A fine dispersion of MWCNTs (0.5 mg) in ethylene glycol monomethyl ether (EGMe) (1.0 g) was prepared using an ultrasonicator (mod. UP400S, Hielscher, Teltow, Germany) fitted with a H_3 sonotrode with a conical geometry. The ultrasonication process was performed according to the following setup: 0.5 cycle and 50 % amplitude for 10 min. The same procedure was used to obtain a dispersion of MCNs (0.15 mg) in EGMe (1.0 g). The MWCNT-EGMe solution (600 μL) and the MCN-EGMe solution (150 μL) were then mixed by an additional ultrasonication cycle (3 min).

Modification of the bare GCE surface was anticipated by mechanical polishing with alumina powder. Three different modifications of the GCE surface were obtained using the MWCNTs dispersion, the MCNs dispersion, and the mixture thereof, so that the MWCNTs/GCE, the MCNs/GCE, and the MWCNT-MCN/GCE modifications were obtained. For all the three modifications, 25 μL of the fine dispersion were displaced on the bare electrode surface. Drying of the coating was performed using an IR lamp (type B, 1440 W, Helios Italquartz srl, Cambiago, Italy) placed 40 cm away from the GCE surface throughout 10 min. The electrode surface was finally rinsed with double-distilled water and stored at 4 °C before usage.

The effective surface area of the MWCNT-MCN/GCE was estimated from the cyclic voltammograms of 1.0 mM $K_3[Fe(CN)_6]$ solution at various scan rates. For a reversible process, the Randles-Sevcik formula (Eq. 3.1) was used (Bard and Faulkner 2001; Nasirizadeh et al. 2011).

$$I_{pa} = 2.69 \times 10^5 \times n^{3/2} A C_0 D^{1/2} \nu^{1/2} \quad (3.1)$$

where I_{pa} refers to the anodic peak current, n the number of electrons transferred, A the surface area of the electrode, D the diffusion coefficient, C_O the concentration of $K_3[Fe(CN)_6]$, and v is the scan rate. For 1.0 mM $K_3[Fe(CN)_6]$ in the 0.1 M KNO_3 electrolyte: $n = 1$ and $D = 7.6 \times 10^{-6}$ cm^2 s^{-1} (Bard and Faulkner 2001; Nasirizadehet et al. 2013), then from the slope of the I_{pa} versus $v^{1/2}$, the effective areas of MWCNT-MCN/GCE was calculated as 0.0653 cm^2.

Electrochemical methods that were conducted in this study are Cyclic Voltammetry (CV), Chronoamperometry (CA), and Amperometry.

3.2.2.2. Electrode Morphology

Morphological views of the electrodes were obtained using a Hitachi S-4800 (Schaumburg, IL) field emission scanning electron microscope (FE-SEM). To this scope, MWCNT/GCE, MCN/GCE, and MWCNT-MCN/ GCE surfaces were first sputtered with Pt/Pd (60/40) for 20 s at a current of 80 mA under an argon atmosphere. Images acquisition was carried out at an acceleration voltage of 1–5 kV and an electrode current of 10 μA.

3.2.2.3. Real Sample Test

The assessment of the modified electrode performance in a real scenario was performed according to the method reported in Ghaani et al. (2018a). Briefly, three-layer pouches (2 dm^2 surface area) made of polyethylene terephthalate (PET, 12 μm thick), polyvinilidene chloride coating (PVDC, 6 μm thick), and low-density polyethylene (LDPE, 50 μm thick), including a PU adhesive, were filled with 100 mL of an acetic acid (3 w/v %) water solution (simulant B). The choice of simulant B accounts for the worst scenario for a possible transfer of PAAs from multilayer packaging materials that include a PU adhesive system. The test was carried out according to a conventional sterilization protocol, that is, at 121 °C for 20 min using an Asal 760 autoclave (Steroglass srl, Perugia, Italy). These conditions were selected with the goal of assessing the effect of high thermal treatments (e.g., pasteurization and sterilization), which have been recently indicated as one potential causes of PAAs formation due to the cleavage of secondary bonds on the main PU backbone (e.g., biuret and especially allophanate bonds) (Campanella et al.

2015). After completion of the sterilization, specific amounts of 2,6-TDA were added in a 20 mL simulant B / PBS solution (1:1) and detected by amperometry, which eventually yielded the final recovery (%) of the analyte.

3.3. Results and Discussion

The detailed results and discussion for this chapter will be given in the following sections.

3.3.1. Morphological characterization of modified glassy carbon electrode (GCEs)

Figure 3.1 displays FE-SEM micrographs of the modified surface of the electrochemical sensors. The modification with MWCNTs yielded a rough morphology (Figure 3.1a) caused by individual and clustered carbon nanotubes (inset of Figure 3.1 a). After modification of the bare GCE with MCNs, spherical particles of 80-100 nm diameter were observed (Figure 3.1b). When the electrode was modified with MWCNTs and MCNs, MWCNTs appeared immersed the spherical domains (Figure 3.1c), with some individual nanotubes pointing out to the medium. (inset of Figure 3.1c).

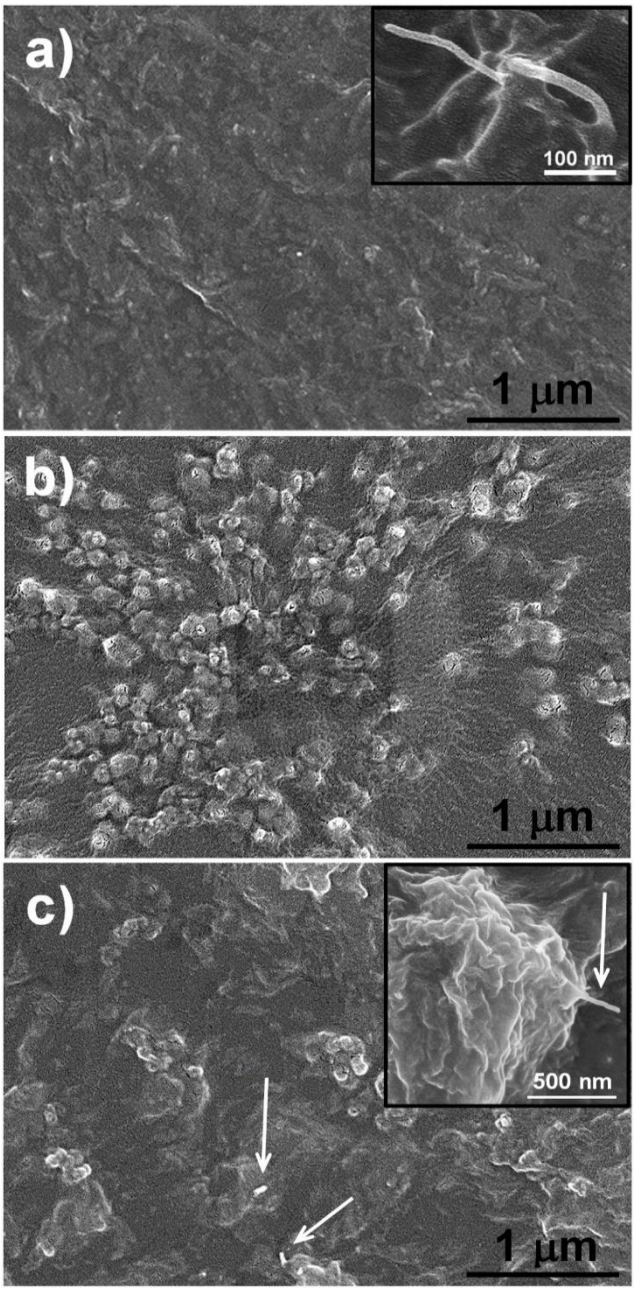

Figure 3.1. FE-SEM surface images of (a) MWCNTs/GCE, (b) MCNs/GCE, and (c) MWCNTs-MCNs/GCE.

3.3.2. Electrochemical Behavior of the Modified Electrode

Cyclic voltammetry (CV) was used to investigate the electrochemical behavior of 2,6-TDA (500 µM) on the surface of both bare and modified electrodes at pH 7.0 (B-R buffer) (Figure 3.2).

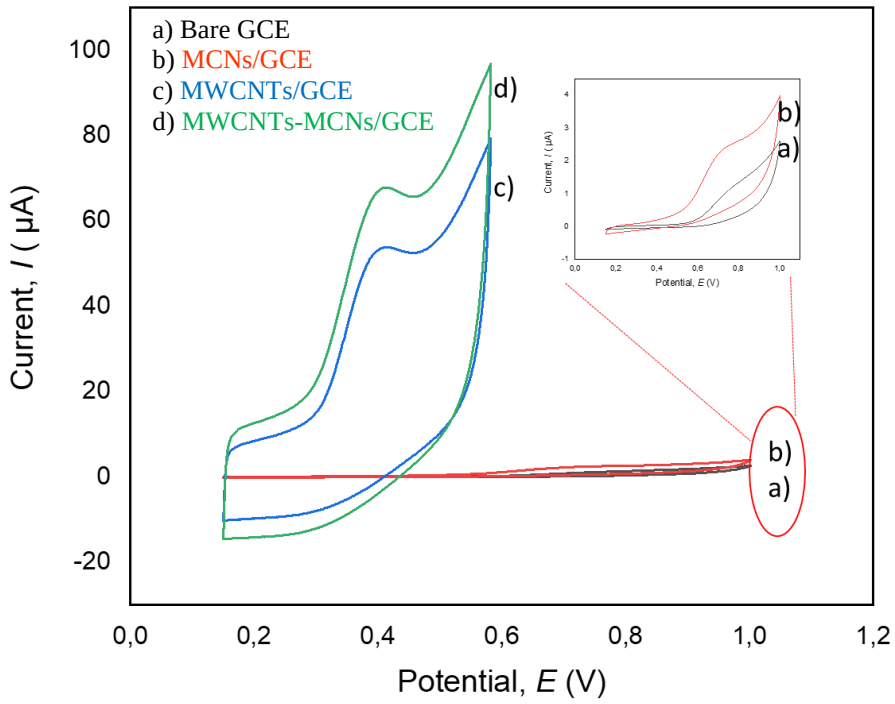

Figure 3.2. Cyclic voltammograms in B-R buffer (pH 7.0) at a 50 mV/s scan rate of (a) bare GCE, (b) MCNs/GCE, (c) MWCNTs/GCE, and (d) MWCNTs-MCNs/GCE in the presence of 500 µM TDA.

The current response of the bare GCE was very weak, as demonstrated by an oxidation peak for 2,6-TDA of 0.079 ± 0.008 µA at 480 mV (Figure 3.2, voltammogram a). Modification with MCNs did not show any significant improvement in the current response (0.527 ± 0.012 µA) compared to the bare electrode (Figure 3.2, voltammogram b), whereas a dramatic increase was measured after modification with MWCNTs, with an oxidation peak of 18.25 ± 0.530 µA (Figure 3.2, voltammogram c). This can be explained in consideration of the two-fold effect arising from the modification, that is, increased surface area and enhanced electron transfer rate of the electrode. As it is shown in Figure 3.2a, the addition of MWCNTs led to a clear change in the surface topography;

that is, the surface of the electrode exposed to the surrounding medium increased due to the tubular MWCNTs pointing out from the surface of the electrode. This explains the dramatic increase in the peak current, as reported before. To corroborate the positive effect of the increased active surface arising from the MWCNTs addition, it is possible to observe the outcome arising from the addition of MCNs (Figure 3.1b). In this case, although the surface topography changed significantly, the peak current did not increase greatly (Figure 3.2, voltammogram b). This can be ascribed to the limited increase of the active electrode surface, which is plausibly due to the lower surface area of MCNs compared to the tubular MWCNTs. The electrochemical performance of the electrode was further improved using MWCNTs in combination with MCNs, with a maximum current response of 20.95 ± 0.750 μA. As shown in Figure 3.2 (voltammogram d), the final output was slightly higher compared to the MWCNTs/GCE, most likely due to the MCNs' remarkable electronic properties, which eventually led to an overall increase in electrode conductivity.

3.3.3. Effect of pH

The pH of the environment surrounding the electrode surface may have an effect on the redox reaction that occurs between the analyte (500 μM) and the modified-GCE. For this reason, CV experiments were performed over the pH range of 5.0–11 in B-R buffer solution. As displayed in Figure 3.3, the maximum oxidation peak current was reached at pH 7. Hence, all the following experiments were conducted at this pH value. It was also observed the linearly inverse relationship between oxidation peak potential and pH; that is, increasing the pH led to a linear decrease of the oxidation peak potential (Figure 3.3). As already noticed (Ghaani et al. 2018a), this observation suggests that the oxidation reaction at the analyte/surface of the electrode interface plausibly involved protons, as corroborated by the linear relationship between the oxidation peak potential and the pH (E_{pa}= -11.084 pH + 475.55, R^2 =0.9518). Finally, a negative shift of the potential by 11.084 mV per pH unit was found.

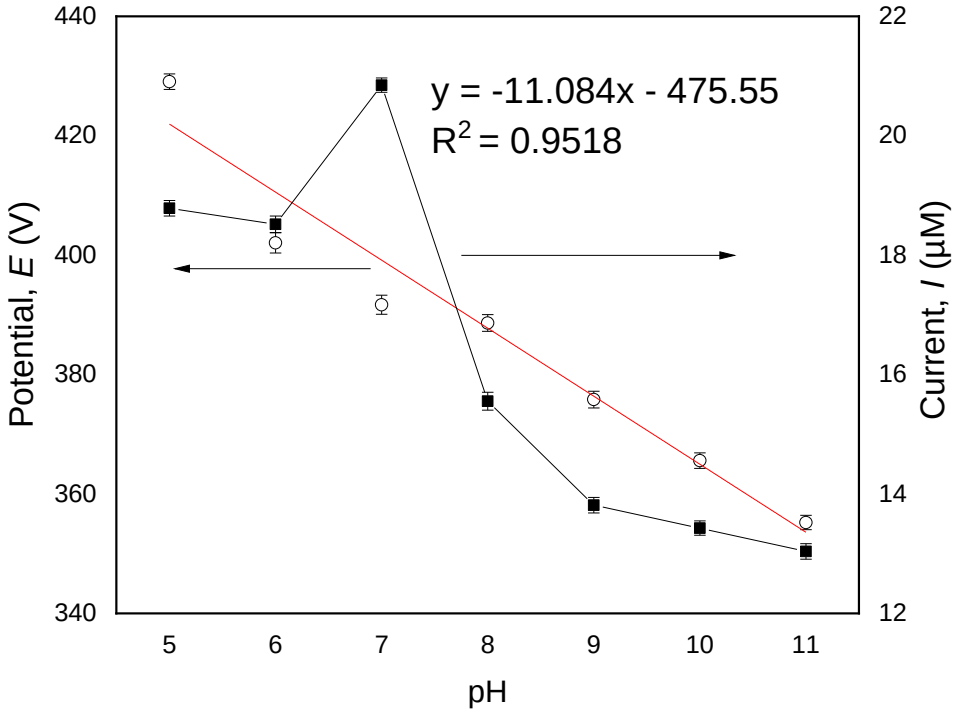

Figure 3.3. Effect of pH (solution containing 500 µM of 2,6-diaminotoluene in 0.1 M Britton-Robinson buffer) on the anodic peak potential (*E*) and current (*I*) of the MWCNTs-MCNs/GC electrode.

3.3.4. Influence of Scan Rate

Information about an electrochemical mechanism can be obtained from the relationship between the peak current and scan rate. We thus investigated the influence of the scan rate on the electrocatalytic oxidation of 2,6-TDA at the MWCNT-MCN/GCE surface with CV within the 5–35 mVs^{-1} range (analyte concentration of 500 µM (Figure 3.4). Each scan rate setting yielded an oxidation peak current (I_p). By plotting the oxidation peak current (I_p) generated by each scan rate setting against the square root of the scan rate, a linear relationship in the 5–35 mVs^{-1} range was established (inset of Figure 3.4). This observation suggests that at a sufficient overpotential the reaction is diffusion limited (Zare, Nasirizadeh, and Mazloum Ardakani 2005).

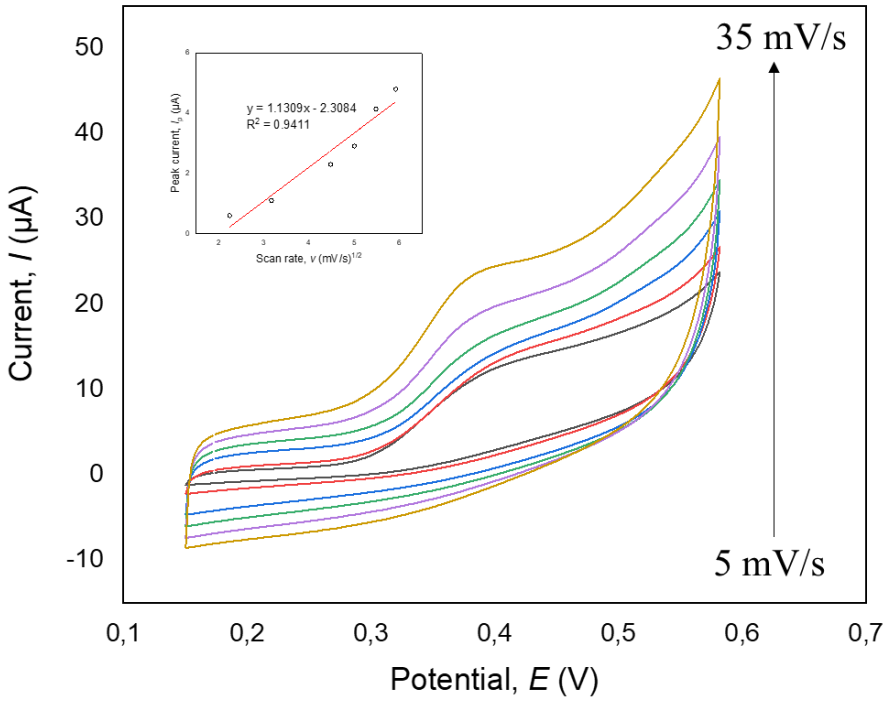

Figure 3.4. Cyclic voltammograms of MWCNTs-MCNs/GCE in B-R buffer (pH 7.0) containing 500μM 2,6-TDA at different scan rates (5-35 mVs^{-1}). The electrocatalytic peak current (I_p) variation as a function of the square root of sweep rate is shown in the inset.

Running CV at different scan rates also allowed to achieve a better understanding of the kinetic mechanism of the GCE surface toward 2,6- TDA. More specifically, applying the Laviron's theory it was possible to calculate the total number of electrons (n) involved in the catalytic reaction using the following equation (Eq. 3.2):

$$E_{pa} = E^0 + \left(\frac{RT}{\alpha nF}\right) ln\left(\frac{RTK^0}{\alpha nF}\right) + \left(\frac{RT}{\alpha NF}\right) lnv \qquad (3.2)$$

where α is the transfer coefficient, K^0 is the standard rate constant of the reaction, n is the electron transfer number, v is the scanning rate, E^0 is the formal redox potential, R is the gas constant, T is the absolute temperature, and F is the faraday constant. Eq. 3.2, which applies for an irreversible electrode process, allowed to find a linear relationship between E_{pa} and ln (v), as expressed by the equation E_p(V) = 0.0399 ln (v) (mVs^{-1}) +

0.2375 (Fig. 3.5), starting from the raw voltammograms reported in Figure 3.5. Using Laviron's equation it was thus possible to calculate the electron transfer number (n), which is given by the slope of E_{pa} versus ln (v) (i.e., $RT/\alpha nF$). Finally, n = 1.17~1 was obtained, which suggests that the electrochemical oxidation of 2,6-TDA at the MWCN-MCN/GCE surface is a one-electron transfer process. This finding differs from what was previously observed for other two PAAs, that is, 4,4'- methylene diphenyl diamine and 2,4-diaminotoluene, for which the oxidation at the surface of a glassy carbon electrode modified with gold nanoparticles, chitosan, and multi-walled carbon nanotubes involved two electrons (Ghaani et al. 2018a; Ghaani et al. 2018b).

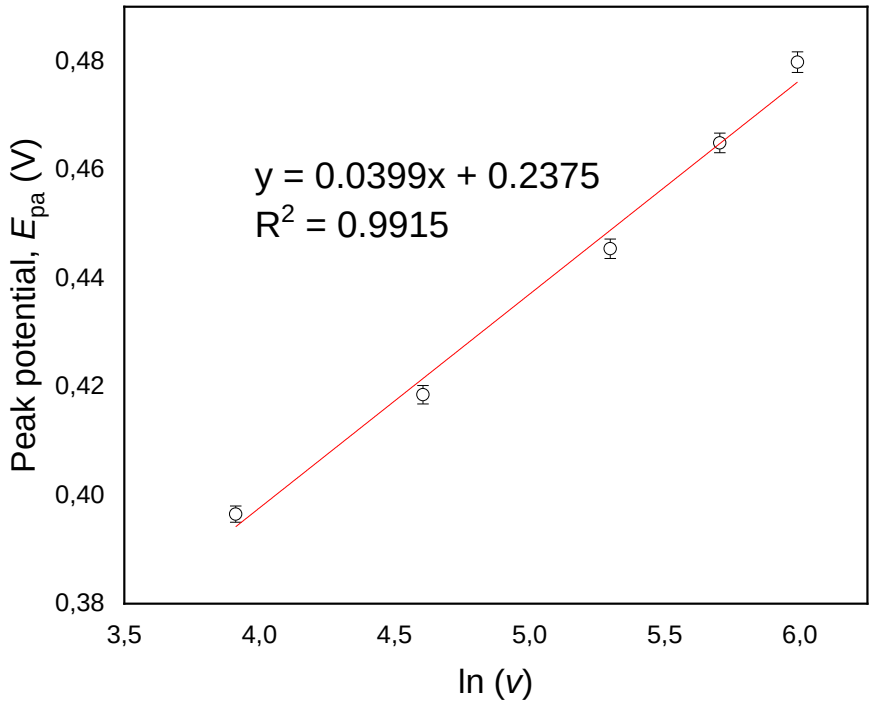

Figure 3.5. Experimental data (empty circles) and linear regression of anodic peak potential (E_{pa}) versus natural logarithm of the scan rate [ln (v)] (50-400 mVs^{-1})

3.3.5. Chronoamperometry measurement

Chronoamperometry experiments were performed to evaluate the electrochemical oxidation of 2,6-TDA. To this scope, chronoamperograms were obtained at a potential step of 480 mV, while the concentration of the analyte was varied between 0.04 and 5 mM at pH 7 (B-R buffer) (Figure 3.6). Cottrell's equation (Eq. 3.3) was used to describe the current response of an electroactive material (such as 2,6-TDA) undergoing a diffusion-limited electrocatalytic process (Bard and Faulkner 2001):

$$I = \frac{nFAD^{1/2}C_b}{\pi^{1/2}t^{1/2}} \tag{3.3}$$

where n is the electron transfer number of (1) exchanged per reactant molecule, F is the Faraday constant (9.648 × 104 $Cmol^{-1}$), A is the geometric area of the electrode (0.0653 cm^2), while C_b ($molcm^{-3}$), and D (cm^2s^{-1}) are the concentration and the diffusion coefficient of 2,6- TDA, respectively.

By plotting *I* against $t^{-1/2}$, different linear curves were obtained moving from 0.04 mM to 5.0 mM 2,6-TDA concentration (Figure 3.6, inset a). The slope of each straight versus 2,6-TDA concentration finally made possible the calculation of the overall slope of the best-fit line (Figure 3.6, inset b) using the following equation:

$$It^{1/2} = \frac{nFAD^{1/2}C_b}{\pi^{1/2}} \tag{3.4}$$

From Eq. (3.4), *D* can be extrapolated according to:

$$D = \frac{(slope)^2\pi}{(nFAC_b)^2} \tag{3.5}$$

Finally, by using the overall slope within Cottrell's equation, an estimate of the average diffusion coefficient was obtained as 1.34×10^{-4} cm^2s^{-1}.

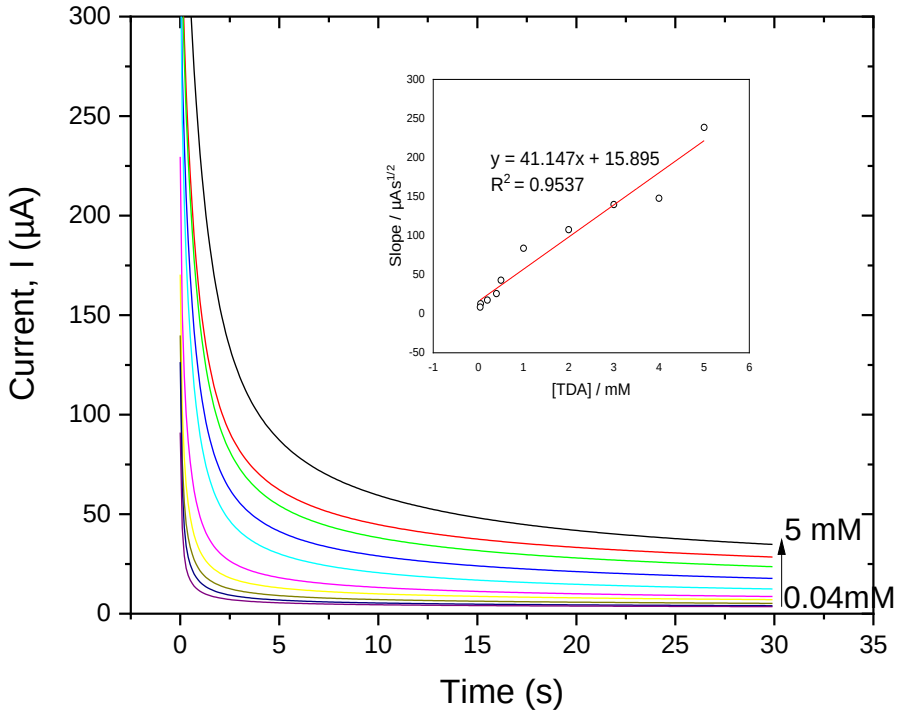

Figure 3.6. Chronoamperograms obtained for the MWCNTs-MCNs/GCE in B-R buffer (pH 7.0) at different concentrations of 2,6-TDA (0.04-5 mM). Inset: plot of the slope of the straight lines against different 2,6-TDA concentrations

3.3.6. Amperiometric test

Amperometry is more widely used than voltammetry to evaluate the sensitivity of a sensor owing to the different mechanism of transfer of the analyte to the electrode surface. Figure 3.7 shows the amperometric response of a rotating MWCNTs-MCNs/GCE after the addition of 2,6-TDA at different concentrations (from 0.53–2326.60 µM) into the 25 mL B-R buffer at the potential step of 450 mV. A positive relationship occurred between the current response and the concentration of 2,6-TDA, with three main linear regions in three wide concentration ranges of 2,6-TDA: 0.53–11.37 µM (Figure 3.7, inset a), 11.37–229.36 µM (Figure 3.7, inset b), and 229.36–2326.60 µM (Figure 3.7, inset c).

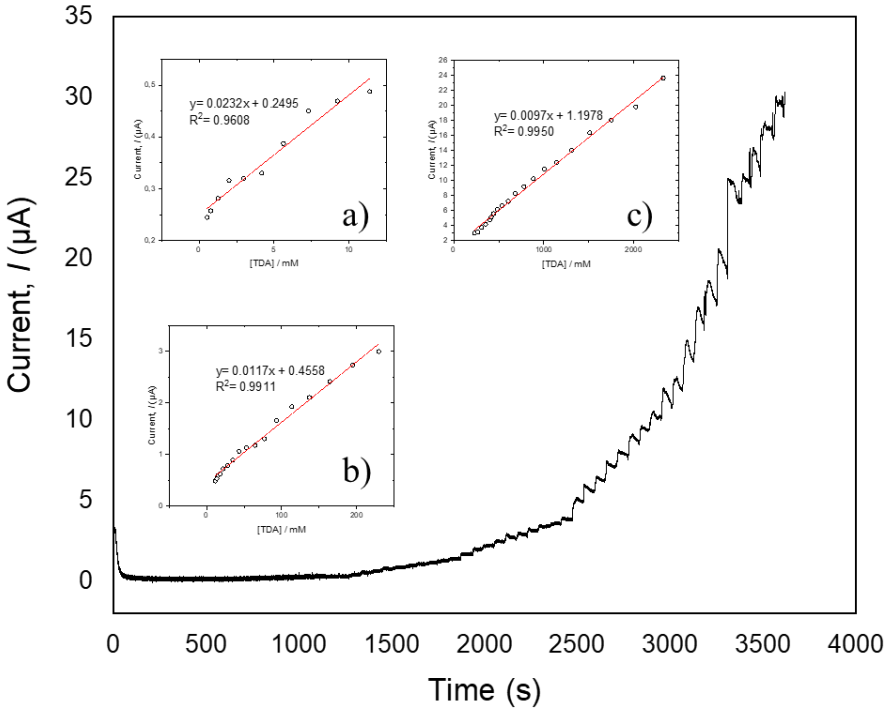

Figure 3.7. Amperometric response at the rotating MWCNTs-MCNs/GCE at 480 mV in 25 mL B-R buffer (pH 7.0) (0.53-2326.60 μM). The variation of the amperometric current against the 2,6-TDA concentration is shown in insets (a) (0.53–11.37 μM), (b) (11.37–229.36 μM) (c) (229.36–2326.60 μM)

The slope of the lower linear range in the amperometric plot was thus used to calculate the sensitivity of the MWCNTs-MCNs/GCE, which was 0.0232 μA $(\mu M)^{-1}$. In turn, the sensitivity of the modified electrode allowed calculating the lower limit of detection of 2,6-TDA, according to the following equation (Shrivastava and Gupta 2011; Skoog, Holler, and Crouch 2007):

$$LOD = \frac{3 \times S_{bl}}{m} \tag{3.6}$$

where S_{bl} is the standard deviation of the current response (μA) obtained from the blank solution (10 replicates) and m is the slope of the before mentioned lower linear range in the amperometric plot. Finally, the calculated LOD value for the MWCNTs-MCNs/GCE was 0.129 μM.

Amperometry experiments were also used to check for the operational stability of the MWCNT-MCN modified electrode. As displayed in the Figure 3.8, no significant differences in the current response of the electrode were observed for ~1280s in the B-R buffer containing 2,6-TDA. This observation supports the fact that there was no inhibitory effect of 2,6-TDA and its oxidation products on the modified electrode surface.

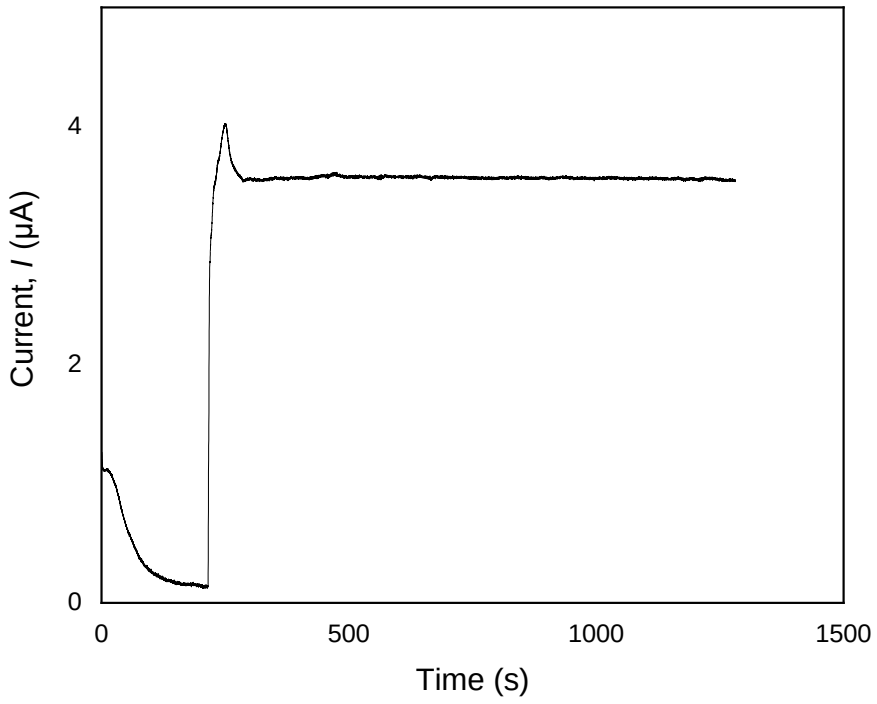

Figure 3.8. The stability of the response of the MWCNTs-MCNs/GCE for 1280s (2,6-TDA concentration 550 μM).

3.3.7. Potential interference of other compounds

The reliability of an electrochemical sensor in real systems can be jeopardized due to interference phenomena, which are caused by the simultaneous presence of electroactive species other than the target analyte in the medium in contact with the electrode surface. If we consider a multilayer packaging material based on PU-adhesives, not only other PAAs, but also a number of additives commonly added during the extrusion process might impair the performance of the electrode due to interference with the target analyte. For this reason, in this work we decided to test the electrocatalytic performance

of the MWCNT-MCN/ GCE toward 2,6-TDA in the presence of various substances as potentially interfering compounds.

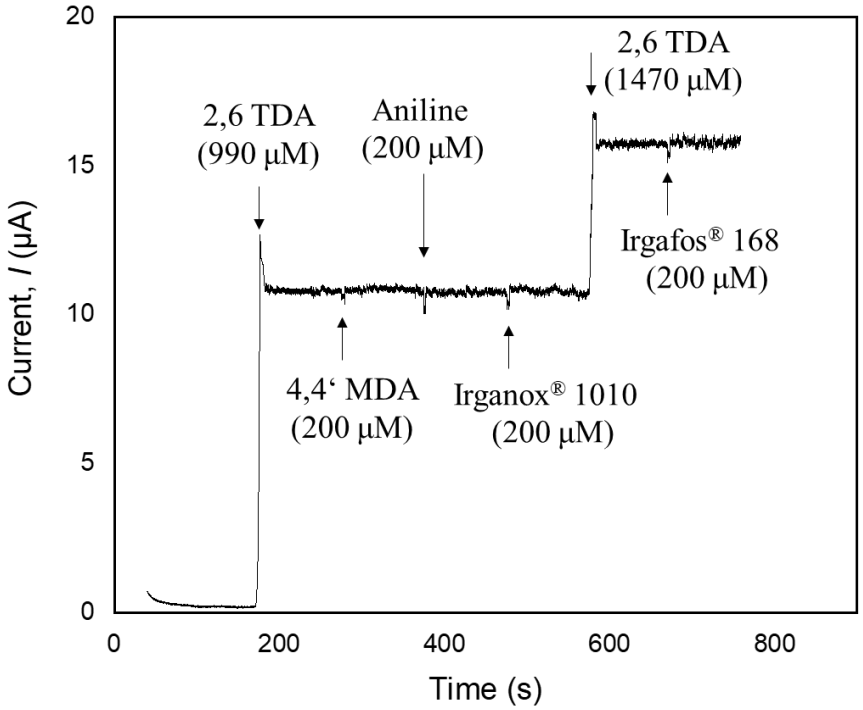

Figure 3.9. Amperometric trace displaying the current response of the MWCNTs-MCNs/GC electrode after the sequential addition of the PAAs 2,6-TDA, 4,4′ - MDA, aniline and the two additives Irganox® 1010 and Irgafos® 168.

At the beginning, aniline and 4,4′-MDA (two other PAAs) were tested. As shown in Figure 3.9, the current response signal did not change when these two PAAs were added (990 μM) to the solution containing 2,6-TDA, demonstrating that both compounds do not interfere with the detection of 2,6-TDA on the MWCNTs-MCNs/GC electrode surface. In a similar way, Irganox® 1010 and Irgafos® 168 (two additives used in the polyolefins manufacturing) were tested. Also in this case, the electrochemical performance of the MWCNT-MCN/GCE was not affected upon the addition of these two additives (200 μM) (Figure 3.9). The outcome of these tests proved that the MWCNT-MCN-modified electrode can be used to quantify selectively the 2,6-TDA.

3.3.8. Real sample test

Real sample tests were carried out using the MWCNTs-MCNs/GCE to demonstrate its capacity for the detection and determination of 2,6-TDA that had possibly formed in packaging materials based on PU adhesives upon migration to the food. To this purpose, the food simulant B (acetic acid water solution, 3 w/v%) was used inside the thermo-sealed pouch, which was then exposed to 121 °C for 20 min (sterilization conditions). The capability of the modified electrode to detect 2,6-TDA was assessed by the standard addition method (Sun and Zhang 2006). As shown in Table 3.1, the modified electrode the MWCNTs-MCNs/GCE performed decidedly well, with a high recovery of the analyte (97.42–106.54 %). This finding clearly indicates that the MWCNTs-MCNs/GCE can be efficiently used to detect the migration of 2,6-TDA that had possibly migrated from multilayer packages that undergo thermal stresses, such as sterilization, pasteurization, microwaving, and sous-vide cooking.

Table 3.1. Amount of added (spiked) and measured 2,6-TDA at the MWCNTs-MCNs/GCE surface, with resulting recovery percentage after the migration test using the food simulant B under typical sterilization conditions (121 °C for 20 min).

Sample	Spiked (μM)	Found (μM)	Recovery (%)
Sample 1	0	-	-
	5.5	5.64	102.54
	35	37.29	106.54
	50	49.36	98.72
Sample 2	0	-	
	5.5	5.42	98.54
	35	34.10	97.42
	50	50.83	101.66
Sample 3	0	-	
	5.5	5.61	102
	35	34.80	99
	50	50.30	100

3.4. Comparison of different analytical methods

Many analytical methods have been developed for the detection and quantification of PAAs. The standard method developed by the German Federal Institute for Consumer Protection and Food Safety is based on a spectrophotometric analysis, as previously reported. However, this method could overestimate PAAs since it determines the sum of all PAAs and can be affected by other substances such as colorants and impurities in the sample (Pezo et al. 2012). To overcome these limitations, other analytical methods with or without preliminary sample preparation steps have been developed for the selective quantification of PAAs. In this context, Aznar et al. developed a method based on solid phase extraction (SPE) followed by LC–MS for the quantification of PAAs possibly migrated from multilayer films to the aqueous food simulant 3% acetic acid (w/v) (Aznar, Canellas, and Nerin 2009). The high recovery range (81–109 %) indicated that this method was adequate for the application to real samples. Moreover, low detection limit, good linearity, and reproducibility were obtained as a result of the analysis. However, preliminary steps, including clean-up and preconcentration, were time consuming, which eventually affected the overall efficiency of the procedure. Furthermore, the recovery of 2,6 TDA, which is one of the PAAs detected by this method, was as high as 93 %, which is lower than that obtained in our study. This method was modified for anaylzing eight primary aromatic amines (m-phenylenediamine, 2,6- and 2,4-toluenediamine, 1,5-diaminonaphthalene, aniline, 4,4'-diaminonaphenylether, 4,4'-methylenedianiline and 3,3' -dimethylbenzidine) without a clean-up process. Even though high recovery and low detection limit were obtained by means of this modified method, many unknown compounds related to primary aromatic amines were also detected, which may cause false-positive results. In comparison to our study, 2,6 TDA was selectively detected and quantified by the MWCNTs/MCNs modified electrode in the presence of other compounds (Sendon et al. 2010). Mortensen et al. reported a method based on a LC/ESI-MS/MS apparatus, with no need for any preliminary step. The final results indicated an excellent accuracy in the determination of twenty primary aromatic amines related to polyurethane products and azo dyes (Mortensen et al. 2005). In another research, a HPLC-(SIM)-MS-based method has been developed to test plastic laminates and recycled paperboards for the migration of PAAs by Lambertini and co-workers (Lambertini et al. 2014). This method exhibited appropriate selectivity, sensitivity, repeatability, and a low detection limit of 0.1–3.6 μg/kg. Even though the relevant method had proper sensitivity

for the detection of twentytwo PAAs, 2,6 TDA was not amongst them. Brede, Skjevrak, and Herikstad (2003) reported that solid phase derivatization as a pretreatment step for GC–MS analysis of possible PAAs migration from packaging materials in water food simulant provided low detection limit of 0.2 μg/kg for 2,6 TDA and good repeatability. Besides, less time and solvent consuming represent other advantages of solid phase derivatization. On the other hand, although these methods have the advantage of high efficient separation, they are very expensive, time-consuming, and highly specialized operators are needed to operate them. In our study, low limit of detection, high recovery of the analyte (97.42–106.54 %), excellent selectivity and stability have been reached by the MWCNTs/MCNs modified electrochemical sensor. Moreover, less time consuming, easiness to use, and relatively low cost of the MWCNTs/MCNs modified sensor makes this approach feasible for routine analysis in a standard packaging laboratory, especially for quality control.

3.5. Conclusion

In this work, we demonstrated how to modify the surface of a GCE to achieve adequate sensitivity and a low limit of detection for the determination of 2,6-TDA, a potential carcinogenic PAAs that can form as a non-intentionally added substances (NIAS) in multilayer packaging materials whereby PU adhesives are used to join the different layers. The proposed modification of the working electrode surface was made using MWCNTs and MCNs, which acted in synergy (increased surface area and enhanced electroconductivity), eventually leading to the excellent electrocatalytic performance of the sensors. This was demonstrated by the outstanding sensitivity, detection limit, and stability of the sensor. Finally, the real samples experiments showed the capability of the MWCNTs-MCNs/GCE to provide reliable results as far as the quantification of 2,6-TDA is concerned. For all the above reasons, the modified sensor proposed in this work may represent an alternative analytical tool to commonly used analytical instrumentation, especially for quality control in industrial plants.

CHAPTER 4

A SCREEN-PRINTED ELECTRODE MODIFIED WITH GOLD NANOPARTICLES/ CELLULOSE NANOCRYSTALS FOR ELECTROCHEMICAL DETECTION OF 4,4´-METHYLENE DIPHENYL DIAMINE

4.1. Introduction

In recent years, to overcome the limitations of conventional analytical methods, smart sensors, specifically screen-printed electrochemical sensors, have attracted considerable attention owing to their ability to replace more complex techniques for detecting a wide range of substances, even in very small amounts (Masawat and Slater 2007). Screen-printed electrodes (SPEs), in particular, are reliable, single-use planar devices that are produced by printing different inks on plastic, glass, or ceramic substrates (Masawat and Slater, 2007). The main advantage of these kinds of electrodes is the miniaturization of a more complex electrochemical setup (which includes a working, reference, and counter electrode in an electrochemical cell) in one device (Kadara, Haggett, and Birch 2006). First, this enables the use of a limited sample volume. In addition, it is possible to adapt the performance of the electrode by modifying the composition of the inks/coatings on its surface according to the specific analyte to be detected. The low cost of SPEs (between 0.7–1.0 €/piece) allows the use of one electrode for each individual measurement so that fouling on the surface of the electrode can be avoided or at least minimized during electrochemical measurement (Renedo, Alonso-Lomillo, and Martinez 2007; Su, Wang, and Cheng 2011). Finally, in spite of their simplicity and ease of use, SPEs afford high reproducibility and sensitivity, and they do not require pre-treatment, such as electrode polishing, as other electrode materials do (Metters, Kadara, and Banks 2011).

As for all electrochemical sensors, in SPEs the applied voltage initiates a redox reaction on the working electrode, resulting in a measurable current proportionate to the

concentration of the target analyte (Ghaani et al. 2018b). However, a bare SPE has low conductivity and low surface area and its surface is susceptible to fouling; these factors can negatively affect the performance of the electrode. Therefore, modification of the electrode surface with metallic nanoparticles and carbon-based nanomaterials has been proposed as one of the most promising options because of large surface area, antifouling and electrocatalytic properties, and high electrical conductivity (Hanssen, Siraj, and Wong 2016; Ghaani et al. 2018a; Viswanathan and Radecki 2008).

This work is the first of its kind because, based on our knowledge, there are no studies investigating SPEs specifically developed to detect PAAs. The main advantage of these novel electrodes is the higher suitability for 'in-field' applications than the conventional electrodes, mainly due to a simpler cell set up. Hence, SPEs modified with appropriate nanomaterials can pave the way for the sensitive, precise, easy, and in-field detection of PAAs. To this goal, a gold nanoparticles-nanocellulose hybrid nanomaterial has been used in this study to modify the surface of the SPE. The combination of AuNPs and CNCs was aimed at achieving remarkable selectivity and a low detection limit for 4,4'-methylene diphenyl diamine (MDA) while preventing fouling on the electrode surface. The final AuNPs/CNCs/SPE was fully characterized and its electrochemical properties were discussed in depth.

4.2. Experimental Study

In the following sections, both materials and methods performed for the quantification of 4,4'-methylene diphenyl diamine (MDA) were given in detail.

4.2.1. Materials

MDA (analytical grade 98%, molar mass 198.26 g mol^{-1}), AuNPs (5 nm diameter), boric acid (99.999% trace metals basis), phosphoric acid (85-90%), aniline (≥ 99.5%), phosphate buffer solution (PBS 0.1 M, pH ~ 7.0), and sulfuric acid (65 vol%) were purchased from Sigma Aldrich (Milan, Italy). Irgafos® 168 [tris (2,4-ditert-butylphenyl)phosphite] and Irganox® 1010 [pentaerythritol tetrakis(3-(3,5-di-tert-butyl-4-hydroxyphenyl)propionate)] were purchased from BASF (Pontecchio Marconi, Italy).

The supporting electrolyte was Britton–Robinson (B–R) universal buffer (0.04 M boric acid, 0.04 M acetic acid, and 0.04 M phosphoric acid) prepared in deionized water.

CNCs were obtained from cellulose of bacterial origin produced according to the procedure proposed in our previous work (Rovera et al. 2018). Briefly, *Komagataeibacter sucrofermentans* DSM 15973 strain (Leibniz Institute DSMZ-German Collection of Microorganisms and Cell Cultures, Braunschweig, Germany) was cultured in a Hestrin and Schramm culture medium (seven days at 30°C) under static conditions. The obtained cellulose pellicles were then soaked for 30 min in a boiling water solution of NaOH 1M to remove residual bacterial cells; this was followed by several washing cycles with distilled water. The bacterial cellulose was then homogenized (15 min at 12,000 rpm) with an Ultra-turrax® T25 Basic mounting a S25 N-18 G dispersing tool (Ika-Werke, Stanfen, Germany). Dehydration was finally performed by freeze-drying at −55°C and 0.63 mbar for 24 h using an ALPHA 1-2 LDplus freeze dryer (Martin Christ, Osterode am Harz, Germany).

CNCs were prepared by adding 1 g of a macrosized bacterial cellulose water dispersion (12 wt.%) to 14 g of sulfuric acid under magnetic stirring (400 rpm) at 55±1°C for 2 h (Rollini et al. 2020). The extraction of CNCs was finalized by the addition of 14 mL cold distilled water followed by centrifugation at 4,000 rpm (2,630 rcf or g-force) for 20 min. CNCs were finally collected as pellets at the bottom of the centrifuge tubes. Excess acid was removed by dialysis, using a cellulosic tube (molecular weight cut-off: 12,000 Da, Sigma-Aldrich, Milan, Italy) against deionized water until neutral pH was achieved.

The Autolab PGSTAT 302N potentiostat (Metrohm, Herisau, Switzerland) with Nova 2.1 software was used for all electrochemical studies. The pH measurements were performed with a BASIC 20+ pH meter (Crison Instruments, S.A. Barcelona, Spain). All of the tests were conducted at a temperature of 25 ± 0.5 °C.

4.2.2. Methods

The methods given below were performed to investigate the behavior of 4,4′-methylene diphenyl diamine (MDA) on the screen-printed electrode surface.

4.2.2.1. Preparation of a modified screen-printed electrode

Commercial SPEs (DropSens C110, Metrohm, Herisau, Switzerland) are electrochemical sensors made of a carbon working electrode (4 mm in diameter), a carbon counter electrode and a silver pseudo-reference electrode. SPEs were modified with CNCs via drop casting. A small volume (6 μL) of CNCs was cast on the working electrode surface and dried for 10 minutes using a double-bulb infrared light (type B, 1440 W, Helios Italquartz srl, Cambiago, Italy) placed at a distance of 40 cm away from the sample. Afterward, AuNPs were used to complete the modifying process. At this stage, 4 μL of AuNPs solution (16.5×10^{12} particles mL^{-1}) were dropped on the surface of the CNCs/SP electrode's surface to obtain the final sensor (AuNPs/CNCs/SPE), which was then dried as previously described. For comparison purpose, CNCs/SP and AuNPs/SP electrodes were also prepared and subjected to investigation.

Cyclic voltammograms using a solution of 1.0 mM $K_3[Fe(CN)_6]$ at various scan speeds allowed the calculation of the effective surface area of the AuNPs/CNCs/SPE. The Randles-Sevcik formula (Eq. 4.1) was utilized for a reversible process (Bard and Faulkner 2001; Nasirizadeh et al. 2011):

$$I_{pa} = 2.69 \times 10^5 n^{3/2} A C_0 D^{1/2} v^{1/2} \quad (4.1)$$

where I_{pa} is the anodic peak current (μA), v is the scan rate (mV s^{-1}), n is the number of electrons transported, A is the electrode surface area (cm^2), D is the diffusion coefficient (cm^2 s^{-1}), and C_0 is the $K_3[Fe(CN)_6]$ concentration (Bard and Faulkner, 2001; Nasirizadeh et al. 2011; Nasirizadeh et al. 2013). The effective mean area of the AuNPs/CNCs/SPE was determined to be 0.176 ± 0.022 cm^2 based on the slope of I_{pa} versus $v^{1/2}$.

Electrochemical methos that were conducted in this study are Cyclic Voltammetry (CV), Chronoamperometry (CA), and Differential Pulse Voltammetry (DPV).

4.2.2.2. Characterization of the surface morphology of the modified electrode

The surface of the CNCs-, AuNPs-, and AuNPs/CNCs-modified SPEs was observed by the use of a field emission scanning electron microscope (FE-SEM, Hitachi

S-4800, Schaumburg, IL). The modified SPEs were first sputtered with Pt/Pd (60/40) for 20 s at a current of 80 mA under an argon atmosphere. Images were captured using a 1–5 kV acceleration voltage and a 10 μA electrode current.

4.2.2.3. Trials on the real packaging films

The performance of the modified electrodes was assessed in a real sample setting (packaging materials consisting polyurethane PU adhesives) using a method published in the work conducted by Ghaani et al. (2018a). Briefly, three-layer pouches (2 dm^2 surface area) made of PET (12 μm thick), EVOH (6 μm thick), and low-density polyethylene (LDPE, 50 μm thick) with a PU adhesive layer (Cartastampa srl, Fornaci di Briosco, Italy) were filled with 100 mL of acetic acid (3 w/v %) water solution (simulant B). This choice accounts for the fact that the worst-case scenario for PAA transfer from multilayer packaging materials with a PU adhesive system was represented by food simulant B (Ghaani et al. 2018a). The experiment was conducted using an Asal 760 autoclave (Steroglass srl, Perugia, Italy) using a conventional sterilization setup (121°C for 20 minutes).

Following the heat treatment, appropriate amounts of MDA were added to 20 mL simulant B/(B-R) universal buffer (1:1) mixture and detected by differential pulse voltammetry (DPV), yielding the final analyte recovery (%).

4.2.2.4. Statistical analysis

Minitab software (version 19.0 for Windows, State College, PA) was used for statistical analyses, and one-way analysis of variance was used to check for differences among samples. The significance level (p) was fixed at 0.05. Unless otherwise stated, all the analyses were performed in triplicate.

4.3. Results and discussion

The detailed results and discussion for this chapter will be given in the following sections.

4.3.1. Morphological characterization of modified SPEs

Figure 4.1 shows the surface morphology of the modified electrodes as revealed by FE-SEM images. In consideration of the fact that the bare electrode surface is very smooth and the FE-SEM image thereof is represented by a flat black background (image not shown), the change in morphology depending on the modification of the bare SPE can be clearly seen. In particular, a fibrillar, rod-shaped morphology was observed in the presence of CNCs (Figure 4.1a), which yielded a visibly rougher surface in comparison to the bare electrode. The deposition of AuNPs led to a typical topography characterized by small nanoparticles clustered in larger domains (Figure 4.1b). However, the presence of AuNPs is hardly visible when they are deposited on top of the CNCs-modified electrode most likely because they were encased in the CNCs framework (Figure 4.1c).

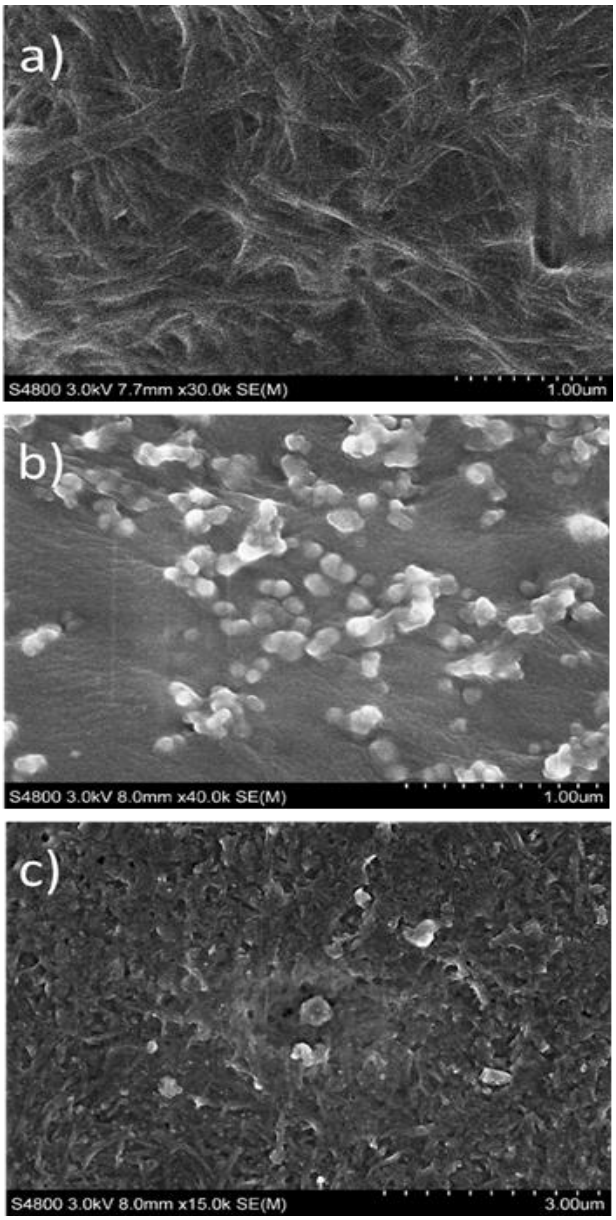

Figure 4.1. FE-SEM surface images of (a) CNCs/SPE, (b) AuNPs/SPE, (c) AuNPs/CNCs/SPE

4.3.2. Electrochemical investigation of MDA oxidation using modified electrodes

The electrochemical behavior of MDA on the surface of differently-modified SPEs was investigated by cyclic voltammetry (CV). Figure 4.2 displays the cyclic voltammetry responses (CV) of the bare SPE, CNCs/SPE, AuNPs/SPE and AuNPs/CNCs/SPE in the presence of 500 μM MDA in a Britton-Robinson (B-R)

universal buffer solution (pH = 7) at a scan rate of 50 mV s^{-1}, whereas the oxidation peaks associated with each curve are reported in Table 4.1.

The weakest peak current response (7.08 μA) was observed from the bare electrode (Figure 4.2a). The modification with only AuNPs (Figure 4.2b) produced a significantly ($p < 0.05$) higher oxidation peak current response of 7.55 μA at the same voltage. This finding proves that AuNPs can increase the conductivity of the SPE to a certain extent. A further improvement was observed after the modification with CNCs, which generated an oxidation peak of 7.99 μA for MDA at the same concentration (Figure 4.2c), thus showing the greater capability of CNCs to increase the surface of the electrode compared to AuNPs, in full agreement with the micrographs of Figure 4.2. Modification of the electrode with both AuNPs and CNCs yielded an additional shift of the CV plot to the highest level (Figure 4.2d), which corresponded to the maximum peak current measured in this work (9.81 μA) (Table 4.1). This increase in the peak current clearly shows the synergistic effect arising from the simultaneous use of CNCs and AuNPs, most likely owing to a simultaneous increase of both the surface area and the electroactivity of the electrode.

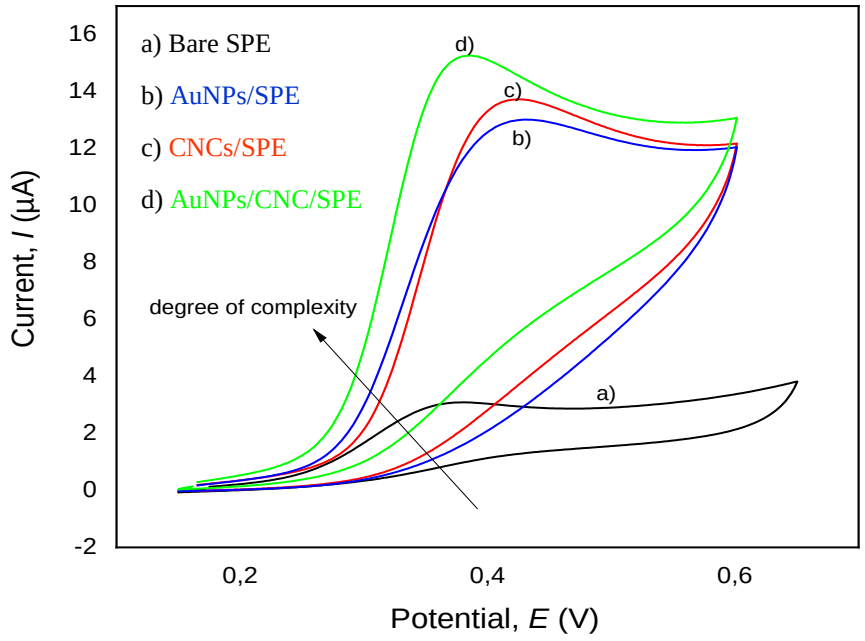

Figure 4.2. Cyclic voltammograms in B-R buffer (pH 7.0) at a 50 mV s^{-1} scan rate of (a) bare SPE, (b) AuNPs/SPE, (c) CNCs/SPE, and (d) AuNPs/CNCs/SPE in the presence of 500 μM MDA

Table 4.1. Evaluation of the oxidation peak current (I_p) of MDA (500 μM) on surface of different modified electrodes at pH = 7.0.

Electrode	Oxidation peak current (μA)	Drying method
Bare SPE	7.08 ± 0.06^{a}	-
AuNPs/SPE	7.55 ± 0.10^{b}	IR lamp
CNCs/SPE	7.99 ± 0.15^{c}	IR lamp
AuNPs/CNCs/ SPE	9.81 ± 0.13^{d}	IR lamp

a-d :Means having different letter within each row denote significant difference at $p<0.05$
Data are mean values ± S.D. (n=3)

Interestingly, the MDA peak current on the bare SPE was greatly higher than the peak current recorded on a bare GCE in the presence of the same analyte (Ghaani et al. 2018a) The same difference was observed by Jin and co-workers when detecting dopamine using both a SPE and a GCE, which was explained in terms of differences in the working electrode structure (Jin, Zhang, and Cheng 2005; Moreno et al. 2010). However, the modification performed on the SPE resulted less effective than the modified GCE, which exhibited a maximum peak current of 25.5 μA. Plausibly, this has to be ascribed to the different modification, which included multi-walled carbon nanotubes (MWCNTs) (Ghaani et al. 2018a), as well as to different operating conditions (e.g., pH of the test).

4.3.3. Effect of pH

The pH level of the medium is one of the most critical factors that greatly affects a sensor's sensitivity. For this reason, CV tests were conducted on our tested electrodes using B-R buffer solutions with a pH ranging between 2 and 11 (Fig. 4.3). The highest oxidation peak current was recorded at pH = 7. As a result, all subsequent studies were carried out at this pH level. This value is lower than the optimum pH value found in the work done by Ghaani et al. (2018). However, this can be due to the different type of sensor used (GCE vs SPE), as also confirmed by Salimi, Mamkhezri, and Hallaj (2006) and Huang et al. (2012), who used different types of electrodes to detect dopamine. Their

findings suggest that the same molecule may exhibit the best oxidation peak at different pH values depending on the electrode type and composition.

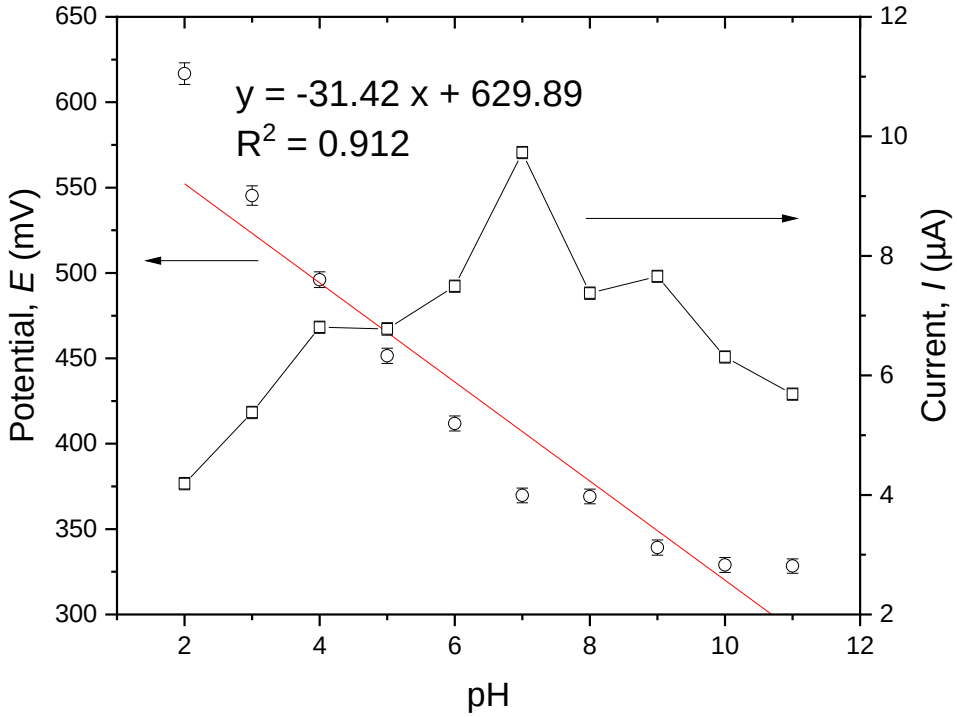

Figure 4.3. Effect of pH value on oxidation peak current and potential of MDA (500 µM) at AuNPs/CNCs/SPE. Scan rate: 50 mV s^{-1}. Electrolyte: 0.1 M B-R buffer

The oxidation peak potential, E_{pa}, decreased according to a quasi-linear trend (E_{pa} = -31.42 pH + 629.89; R^2 = 0.912) as the pH was increased, thus suggesting the active involvement of protons in the MDA oxidation reaction. According to the previously shown linear regression equation, the oxidation peak potential is shifted downward by 31.42 mV per pH unit. Based on the Nernst equation, a slope of 0.0592/2 shows a proton-to-electron ratio of 2:1, implying that one proton for every two electrons was engaged in the electrochemical for MDA oxidation.

4.3.4. Influence of scan rate

Figure 4.4 displays the CVs of 500 µM MDA in B-R buffer solution at various scan rates (10-45 mV s^{-1}). The findings indicated that as the square root of scan rate was increased, the peak current increased linearly. Additionally, it was discovered that the

relationship between peak height (I_p) and the square root of scan rate ($v^{1/2}$) was linear, indicating that, at appropriate overpotential, the process is diffusion rather than surface controlled (inset of Figure 4.4).

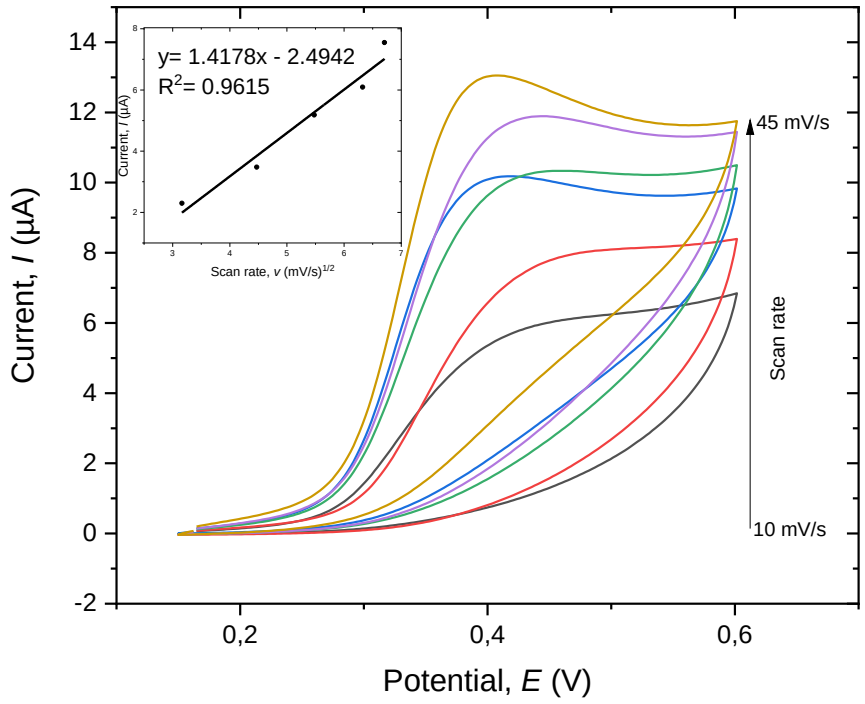

Figure 4.4. Cyclic voltammograms of AuNPs/CNCs/SPE in B-R buffer (pH 7.0) including 500 µM MDA at various scan rates (10-45 mV s^{-1}). Inset displays anodic peak current vs. $v^{1/2}$

The sum of all the electrons (n) used in the entire catalytic process can be calculated using Laviron's theory, which is an appropriate technique for investigating the kinetic mechanism of the electrode with respect to the analyte. As a result, the following equation (Eq. 4. 2) for a completely irreversible electrode process may be used to describe the anodic peak potential (E_{pa}) as a function of the scan rate's natural logarithm (ln v) Laviron 1974):

$$E_{pa} = E^0 + \left(\frac{RT}{\alpha nF}\right) ln\left(\frac{RTK^0}{\alpha nF}\right) + \left(\frac{RT}{\alpha nF}\right) lnv \qquad (4.2)$$

where α is the transfer coefficient, n is the electron transfer number, υ is the scanning rate, E^0 is the formal redox potential, R is the gas constant (8.314 J mol^{-1} K^{-1}),

T is the absolute temperature, and *F* is the Faraday constant (9.648×10^4 C mol^{-1}). It is worth noting that the elaboration of data contained in the raw voltammograms presented in Figure 4.4 perfectly fit the mathematical relationship expressed by Eq. (2), thus allowing the discovery of a linear relationship between E_{pa} and ln (v), as showed by the equation E_p(V) = 0.024 ln (v) (mV s^{-1}) + 0.3454 (Figure 4.5). The slope of E_{pa} vs ln (v), which is RT/nF, can be used to calculate the electron transfer number (n) using Laviron's equation. After the proper substitutions, the final value of n 2.14 ≈ 2 was achieved; demonstrating that a two-electron transfer mechanism is involved in the electrochemical oxidation of MDA at the AuNPs/CNCs modified SPE.

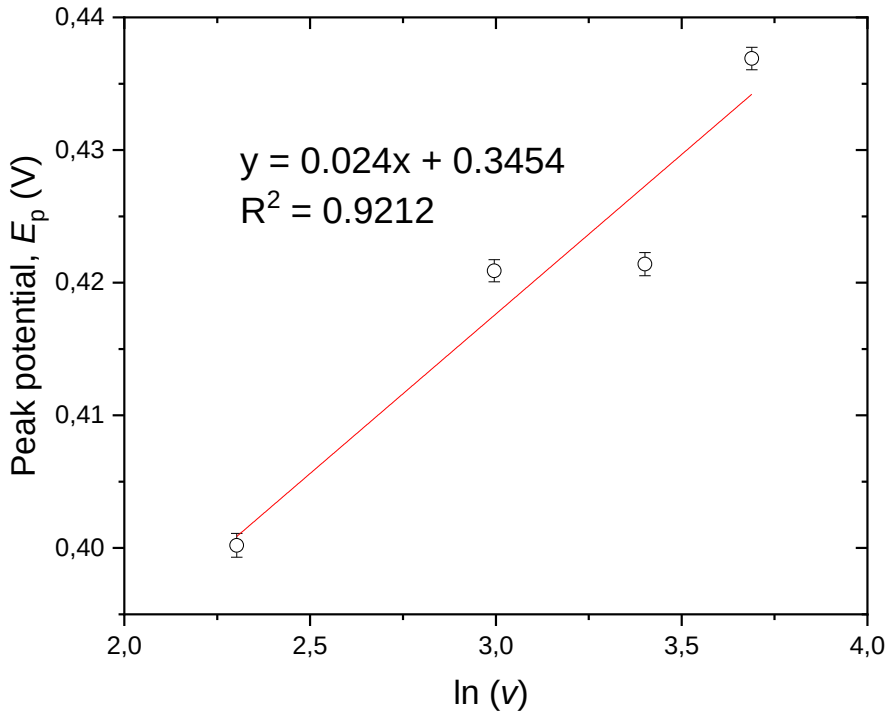

Figure 4.5. The relationship between the peak potentials (E_p) and the natural logarithm of scan rates (ln v) for MDA (10-45 mV s^{-1}).

4.3.5. Chronoamperometry measurements

To gain additional insight into the electrochemical oxidation of MDA on the surface of AuNPs/CNCs/SPEs, chronoamperometric studies were executed by fixing the potential of the electrode at 550 mV and testing solutions with various concentrations of MDA, from 0.02 mM to 1.2 mM in B-R buffer (Fig. 4.6).

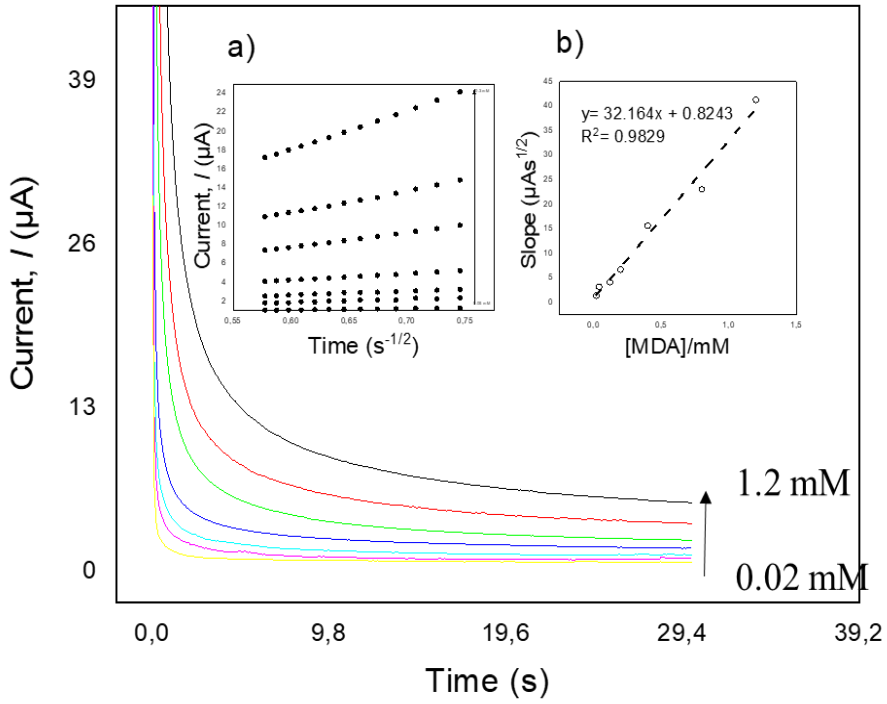

Figure 4.6. Chronoamperograms obtained at AuNPs/CNCs/SPE in B-R buffer solution (pH 7.0) for various MDA concentrations (0.02-1.2 mM). Insets: (a) Plots of I vs. $t^{-1/2}$ gained from the chronoamperograms. (b) Plot of the slope of the straight lines against MDA concentration. (0.02-1.2 mM).

For an electroactive material with a diffusion coefficient D, the current response under diffusion control is described by the Cottrell equation (Eq. 4.3):

$$I = \frac{nFAD^{1/2}C_b}{\pi^{1/2}t^{1/2}} \tag{4.3}$$

while n is equal to 2, which represents how many electron exchanges there are in each reactant molecule, F is the Faraday constant, A is the electrode effective surface area (0.176 cm^2), t is the observation time (s), C_b (mol cm^{-3}) is the concentration of MDA and D (cm^2 s^{-1}) is the diffusion coefficient of MDA.

Different linear curves were generated by plotting I against $t^{-1/2}$ for MDA concentrations ranging from 0.02 mM to 1.2 mM (Fig. 4.6a). The slope of each straight line versus MDA concentration allowed the total slope of the best-fit line (Fig. 4.6b) to be calculated using Eq. (4.4):

$$It^{1/2} = \frac{nFAD^{1/2}C_b}{\pi^{1/2}} \quad (4.4)$$

In particular, *D* can thus be drawn from Eq. (4.5):

$$D = \frac{(slope)^2\pi}{(nFAC_b)^2} \quad (4.5)$$

Within the Cottrell equation, the overall slope was employed to get a diffusion coefficient of 2.82 × 10^{-6} cm^2 s^{-1}. This value is lower than the coefficient of diffusion calculated in the case of a modified GCE (9.49 × 10^{-5} cm^2 s^{-1}) (Ghaani et al. 2018a), which plausibly reflects the different mechanism of transfer due to both type of electrode and nature of the modification.

4.3.6. Differential pulse voltammetric studies

In this work, the sensitivity of the AuNPs/CNCs screen-printed electrode to MDA was investigated by differential pulse voltammetry (DPV). To obtain the DP voltammograms of MDA, appropriate volumes of the stock solutions of MDA were added to the cell containing B-R buffer (9 mL) for a total volume of 10 mL. Figure 4.7 shows the voltammetric response of MDA at different concentrations. The calibration curve of MDA was linear across a single concentration range (0.12-100 μM) (inset of Figure 4.7). The proposed sensor's lower limit of detection (LOD) was computed using the subsequent equation (Eq. 4.6):

$$LOD = \frac{3\times S_{bl}}{m} \quad (4.6)$$

where the slope of the linear range in the voltammetric plot (*m*) was 0.0576 A $(M)^{-1}$ and S_{bl} is the current response's standard deviation (μA) calculated from the blank solution (10 repetitions). Eventually, the AuNPs/CNCs/SPE LOD value was calculated to be 0.057 μM.

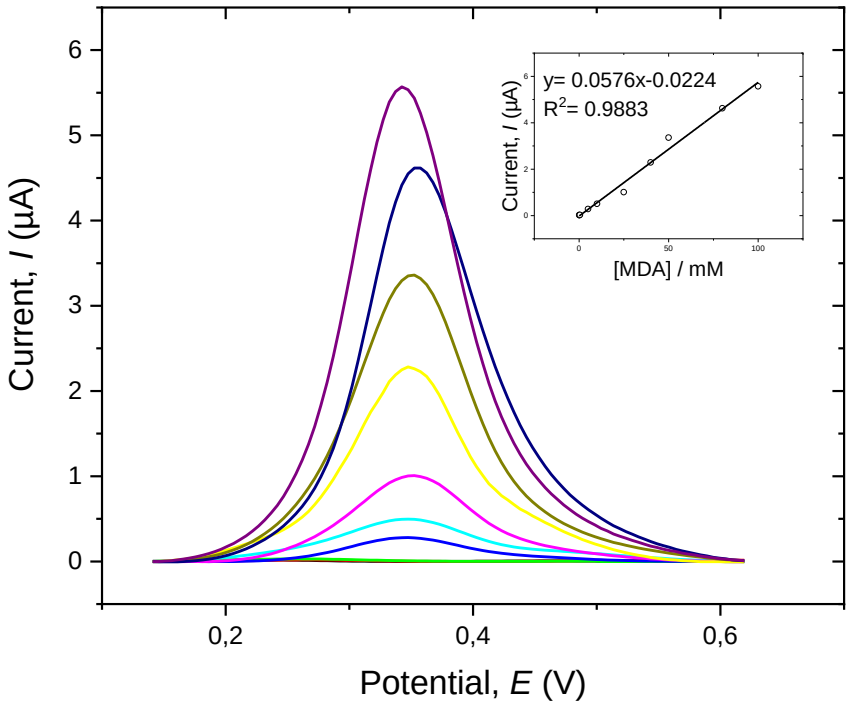

Figure 4.7. Differential pulse voltammetry response of AuNPs/CNCs/SPE in 10 mL B-R buffer (pH = 7.0) containing different concentrations of MDA (0.12-100 µM). Inset: Plot of MDA concentrations versus peak current

A comparison of our work with the study carried out by Ghaani et al. shows that the modified GCE had a lower LOD than the modified SPE of this study (AuNPs/CNCs/SPE) (Ghaani et al. 2018a), somehow in line with our previous observations on the higher performance of a GCE system. As reported in the literature, a higher LOD of modified SPEs compared to modified GCEs was confirmed by other authors. For example, the LOD of a GCE modified with MWCNTs-AuNPs for bisphenol A was 7.5 nM (Tu et al. 2009), while the LOD of a magnetic-activated carbon-cobalt modified SPE for the same analyte was 10 nM (Emambakhsh et al. 2022). Jin et al. (2005) found a LOD of 20 nM for the dopamine detection using a poly (p-aminobenzene sulfonic acid)-modified GCE, whereas Moreno et al. (2010) calculated a LOD of 60 nM for dopamine on graphene quantum dots/ionic liquid-modified SPE. Interestingly, both a GCE and a SPE with the same modification were used for the detection of catechol (Talarico et al. 2015; Lounasvuori, Kelly, and Foord 2018). LOD values were found at

41 nM and 100 nM, respectively. According to this strict comparison, GCEs seem to achieve a lower detection limit than SPEs.

4.3.7. Possible interference of other substances

Interference effects generated by the simultaneous presence of electroactive compounds in the target solution can affect adversely the performance of the sensor. In the case of a multilayer packaging material including PU adhesives, a variety of additives routinely applied during the extrusion process may decrease electrode performance due to interference with the target analyte. As a result, we examined the electrocatalytic efficacy of the AuNPs/CNCs/SPE against MDA in the presence of a variety of possibly interfering chemicals in this study.

The modified screen-printed electrode's anti-interference ability was tested against two additives commonly used in polyolefins, Irganox® 1010 and Irgafos® 168. DPV experiments (data not shown) revealed that no increase in the current response was observed after the addition of these compounds (40 μM) to the MDA containing solution, demonstrating that the fabricated sensor is proper for selective MDA detection.

Lastly, a relative standard deviation (RSD) of 3.65 % was obtained from the single modified electrode (AuNPs/CNCs/SPE) used for five consecutive measurements in the same MDA solution (10 μM), demonstrating the sensor's high repeatability. Also, the reproducibility of the proposed sensor was investigated through DP voltammograms at 10 μM MDA using five distinct sensors (AuNPs/CNCs/SPE). The measured RSD (4.20 %) indicates good reproducibility of the fabricated sensor.

4.3.8. Real sample analysis

The AuNPs/CNCs/SP electrodes were used in real sample experiments to show their ability to detect and determine MDA that had possibly formed in packaging materials based on PU adhesives. For this purpose, food simulant B (3 w/v % acetic acid water solution) was employed within a thermo-sealed pouch that was subsequently subjected to 121 °C for 20 minutes (sterilization conditions). The conventional addition model was used to evaluate the modified electrode's ability to detect MDA. As can be seen in Table 4.1, the AuNPs/CNCs-modified electrode worked efficiently, with high

recovery (98.20–104.07 %). This result clearly shows that the AuNPs/CNCs/SPE may be utilized to detect MDA migration from multilayer packages that have been subjected to thermal stresses. SPE's recovery was slightly higher than GCE's, which is consistent with other studies (Ghaani et al. 2018a; Tu et al. 2009; Emambakhsh et al. 2022).

Table 4.2. Determination and recovery of MDA in a food simulant B sample using AuNPs/CNCs/SPE

Sample	Spiked (μM)	Found (μM)	Recovery (%)
Laminate structure (PET/EVOH/LDPE) including a PU adhesive	0	-	-
	5	4.91	98.20
	40	41.63	104.07
	80	79.02	98.77

4.4. Conclusion

In this work, the detection of MDA, which ranks among the most significant PAAs that might contaminate foods by migrating from multilayer packaging materials created with PU adhesives, was performed by a screen-printed electrode modified with CNCs and AuNPs. The interaction between CNCs and AuNPs with regard to the electro-oxidation of MDA was highlighted as the primary element that causes the superior sensitivity of the sensor and absence of fouling when compared with the bare SPE. Lastly, the real sample trials demonstrated the AuNPs/CNCs/SPE's ability to deliver consistent data in the quantification of MDA. For these reasons, the proposed sensor could be a viable alternative to routinely used analytical instrumentation, particularly for quality control in industrial operations.

CHAPTER 5

DEVELOPMENT OF A NAN0-MODIFIED SCREEN PRINTED ELECTRODE FOR THE DETERMINATION OF 2,4-DIAMINOTOLUENE (TDA)

5.1. Introduction

2,4-diaminotoluene (2,4-TDA) is one of the most important primary aromatic amines that can transfer from packaging materials produced using polyurethane adhesives and can cause severe negative health impacts on human. In this regard, their rapid, sensitive, selective and reliable detection and quantification have great importance in terms of food quality and safety (Ghaani et al. 2018; Campanella et al. 2015).

In this chapter, a screen-printed electrode was developed for the detection of one of the most important primary aromatic amines, 2,4 TDA. In order to increase the selectivity of the sensor against the target analyte, electrode surface was modified by gold nanoparticle (AuNPs) and cellulose nanocrystals (CNCs) solution, and a comprehensive electrochemical characterization was done to investigate the electrochemical properties of 2,4-TDA on the modified electrode surface. A migration test was also conducted to evaluate nano-modified sensor performance in real systems.

5.2. Experimental Study

In the following sections, both materials and methods performed for the quantification of 2,4 TDA were given in detail.

5.2.1. Materials

2,4 TDA (analytical grade 98%, molar mass 122.171 g mol^{-1}), AuNPs (5 nm diameter), boric acid (99.999% trace metals basis), phosphoric acid (85-90%), aniline (≥ 99.5%), phosphate buffer solution (PBS 0.1 M, pH ~ 7.0), and sulfuric acid (65 vol%) were purchased from Sigma Aldrich (Milan, Italy). Irgafos® 168 [tris (2,4-ditert-

butylphenyl)phosphite] and Irganox® 1010 [pentaerythritol tetrakis(3-(3,5-di-tert-butyl-4-hydroxyphenyl)propionate)] were purchased from BASF (Pontecchio Marconi, Italy). The supporting electrolyte was Britton–Robinson (B–R) universal buffer (0.04 M boric acid, 0.04 M acetic acid, and 0.04 M phosphoric acid) prepared in deionized water.

CNCs were obtained from cellulose of bacterial origin produced according to the procedure proposed in the previous chapter (Rovera et al. 2018). Briefly, *Komagataeibacter sucrofermentans* DSM 15973 strain (Leibniz Institute DSMZ-German Collection of Microorganisms and Cell Cultures, Braunschweig, Germany) was cultured in a Hestrin and Schramm culture medium (seven days at 30°C) under static conditions. The obtained cellulose pellicles were then soaked for 30 min in a boiling water solution of NaOH 1M to remove residual bacterial cells; this was followed by several washing cycles with distilled water. The bacterial cellulose was then homogenized (15 min at 12,000 rpm) with an Ultra-turrax® T25 Basic mounting a S25 N-18 G dispersing tool (Ika-Werke, Stanfen, Germany). Dehydration was finally performed by freeze-drying at −55°C and 0.63 mbar for 24 h using an ALPHA 1-2 LDplus freeze dryer (Martin Christ, Osterode am Harz, Germany).

CNCs were prepared by adding 1 g of a macrosized bacterial cellulose water dispersion (12 wt.%) to 14 g of sulfuric acid under magnetic stirring (400 rpm) at 55±1°C for 2 h (Rollini et al., 2020). The extraction of CNCs was finalized by the addition of 14 mL cold distilled water followed by centrifugation at 4,000 rpm (2,630 rcf or g-force) for 20 min. CNCs were finally collected as pellets at the bottom of the centrifuge tubes. Excess acid was removed by dialysis, using a cellulosic tube (molecular weight cut-off: 12,000 Da, Sigma-Aldrich, Milan, Italy) against deionized water until neutral pH was achieved.

The Autolab PGSTAT 302N potentiostat (Metrohm, Herisau, Switzerland) with Nova 2.1 software was used for all electrochemical studies. The pH measurements were performed with a BASIC 20+ pH meter (Crison Instruments, S.A. Barcelona, Spain). All of the tests were conducted at a temperature of 25 ± 0.5 °C.

5.2.2. Methods

The methods given below were performed to evalaute the behavior of 2,4-diaminotoluene (TDA) on the screen-printed electrode surface.

5.2.2.1. Preparation of a modified screen-printed electrode

Screen-printed electrodes (DropSens C110, Metrohm, Herisau, Switzerland), having working electrode, a carbon counter electrode and a silver pseudo-reference electrode, were modified with AuNPs-CNCs via drop casting. 600 µL of AuNPs solution was mixed with 200 µL of CNCs solution. A small volume (6 µL) of this mixture was cast on the working electrode surface and dried for 10 minutes under a double-bulb infrared light (type B, 1440 W, Helios Italquartz srl, Cambiago, Italy) placed at a distance of 40 cm from the sample. For comparison purpose, CNCs/SP and AuNPs/SP electrodes were also prepared and evaluated.

Surface area of the modified electrode was determined as described in the previous chapter. Briefly, cyclic voltammograms using a solution of 1.0 mM $K_3[Fe(CN)_6]$ at various scan speeds was conducted to calculate effective surface area of the AuNPs-CNCs/SPE. The Randles-Sevcik formula (Eq. 5.1) was utilized for a reversible process (Bard and Faulker 2001; Nasirizadeh et al. 2011):

$$I_{pa} = 2.69 \times 10^5 n^{3/2} A C_0 D^{1/2} v^{1/2} \quad (5.1)$$

where I_{pa} is the anodic peak current (µA), v is the scan rate (mV s^{-1}), n is the number of electrons transported, A is the electrode surface area (cm^2), D is the diffusion coefficient (cm^2 s^{-1}), and C_0 is the $K_3[Fe(CN)_6]$ concentration (Bard and Faulker, 2001; Nasirizadeh et al. 2011; Nasirizadeh et al. 2013). The effective mean area of the AuNPs-CNCs/SPE was determined to be 0.181 ± 0.045 cm^2 based on the slope of I_{pa} versus $v^{1/2}$.

Electrochemical methos that were conducted in this study are Cyclic Voltammetry (CV), Chronoamperometry (CA) and Differential Pulse Voltammetry (DPV).

5.2.2.2. Morphological characterization of the electrode surface

The surface of the CNCs-, AuNPs-, and AuNPs-CNCs-modified SPEs was observed using a field emission scanning electron microscope (FE-SEM, Hitachi S-4800, Schaumburg, IL). The modified SPEs were first sputtered with Pt/Pd (60/40) for 20 s at a current of 80 mA under an argon atmosphere. Images were captured using a 1–5 kV acceleration voltage and a 10 μA electrode current.

5.2.2.3. Tests on real multilayer packaging materials

In order to assess the performance of modified electrode in real systems a migration test was conducted as described by Ghaani et al., (2018). In brief, three-layer pouches (2 dm^2 surface area) made of PET (12 μm thick), EVOH (6 μm thick), and low-density polyethylene (LDPE, 50 μm thick) with a PU adhesive layer (Cartastampa srl, Fornaci di Briosco, Italy) were filled with 100 mL of acetic acid (3 w/v %) water solution (simulant B) to simulate the worst-case scenario for PAA transfer from multilayer packaging materials with a PU adhesive system was represented by food simulant B Ghaani et al. (2018a). The experiment was conducted using an Asal 760 autoclave (Steroglass srl, Perugia, Italy) at sterilization conditions (121°C for 20 minutes).

Following the sterilization, proper amounts of 2,4-TDA were added to 20 mL simulant B/(B-R) universal buffer (1:1) mixture and detected by differential pulse voltammetry (DPV) to find out the final analyte recovery (%).

5.2.2.4. Statistical analysis

Data were analyzed using Minitab software (version 19.0 for Windows, State College, PA) and one-way analysis of variance was applied to check for differences among samples. The significance level (*p*) was fixed at 0.05. Unless otherwise stated, all the analyses were performed in triplicate.

5.3. Results and discussion

The detailed results and discussion for this chapter will be given in the following sections.

5.3.1. Morphological characterization of modified screen-printed electrodes (SPEs)

The surface morphology of the modified electrodes was evaluated by FE-SEM, as indicated in Figure 5.1. Given that the surface of the bare electrode is highly smooth and that its FE-SEM image has a flat black background (image not shown), the morphological change resulting from the modification of the bare SPE can be clearly observed. As mentioned in the previous chapter, modifying the electrode surface with CNCs (Figure 5.1 a) caused a rougher surface when compared to the bare electrode. Small nanoparticles clustered in larger domains was observed in the SEM images of the AuNPs modified electrode (Figure 5.1b). When the eeectrode surface was modified with the mixture of AuNPs and CNCs, AuNPs were wrapped in the CNCs phase, and both the needle-like shape of CNCs and the round shape of AuNPs became hardly visible (Figure 5.1c).

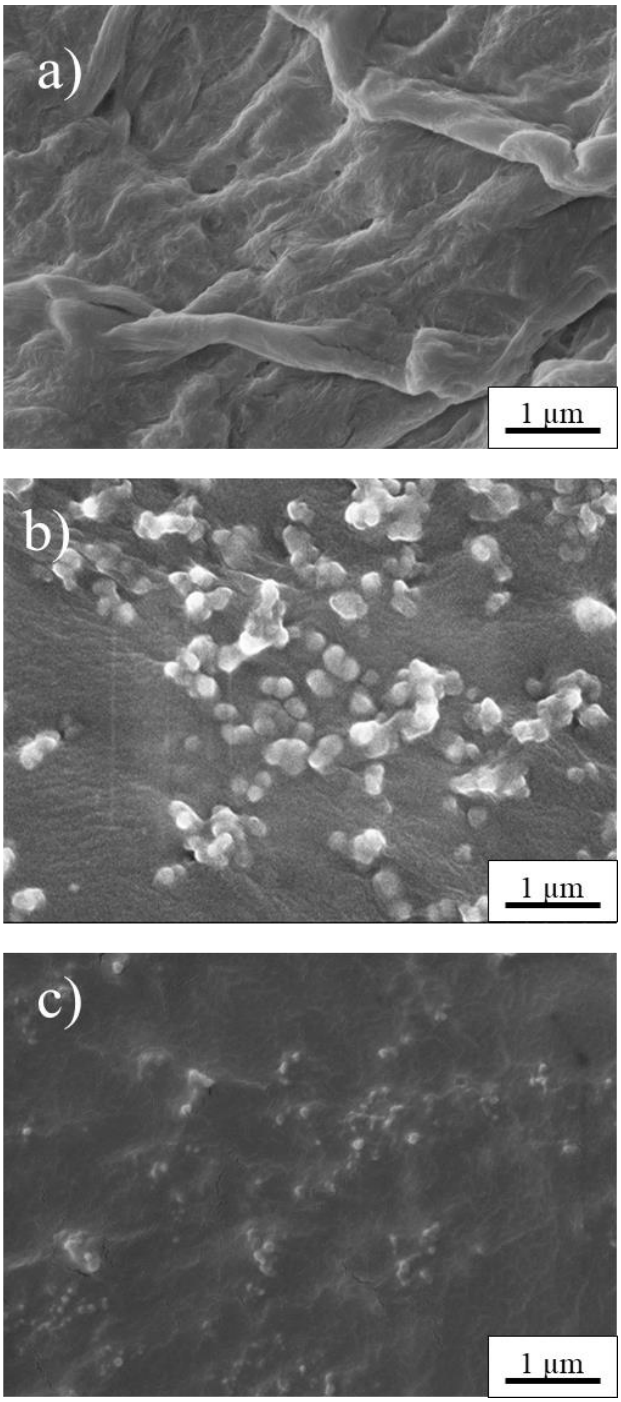

Figure 5.1. FE-SEM images of a) CNCs/SPE, b) AuNPs/SPE, and c) AuNPs-CNCs/SPE

5.3.2. Electrochemical behavior of 2,4 TDA on electrode surface

The electrochemical behavior of both bare and modified electrodes was examined by cyclic voltammetry (CV). Figure 5.2 represents the CV response obtained for the bare SPE (a) and the electrode modified with AuNPs (b), CNCs (c) and AuNPs-CNCs (d) in

the presence of 500 µM 2,4-TDA in B-R Buffer at a scan rate of 50 mVs^{-1}. Table 5.1 indicates the oxidation peaks corresponding to each curve.

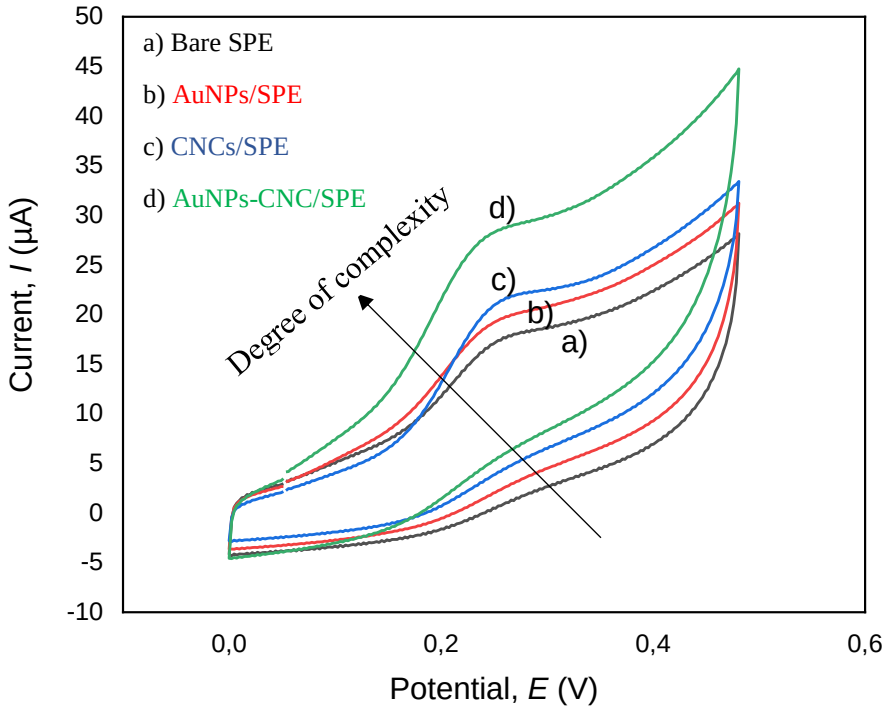

Figure 5.2. Cyclic voltammograms in B-R buffer (pH 7.0) at a 50 mVs^{-1} scan rate of (a) bare SPE, (b) AuNPs/SPE, (c) CNCs/SPE, (d) AuNPs-CNCs /SPE in the presence of 500 µM 2,4-TDA

The bare SPE indicated a weak oxidation peak with a low current (Figure 5.2 voltammogram a). The modification with only AuNPs (Figure 5.2 voltammogram b) did not create a higher oxidation peak current response when compared to that of bare electrode at the same voltage. According to the voltammogram c in Figure 5.2, the oxidation peak current increased remarkably ($p < 0.05$) after modification with CNCs, thus showing the greater capability of CNCs to increase the surface of the electrode compared to AuNPs, in full agreement with the micrographs of Figure 5.1.

In order to improve the performance of the electrode, a mixture of AuNPs and CNCs was used in the final step. Modification of the electrode with a mixture of AuNPs and CNCs provided an additional shift in the CV plot to the highest level (Figure 5.2 voltammogram d) corresponding to the maximum peak current (7.22 µA) measured in this study (Table 5.1). It can be concluded that modification of the electrode with the

mixture of AuNPs and CNCs most probably increased the surface area and electroactivity of the electrode and lead to an increase in peak current.

Table 5.1. Comparison of the oxidation peak current (I_p) of 2,4-TDA on various electrode surfaces at pH = 7.0

Electrode	Oxidation peak current (μA)	Drying method
Bare SPE	3.46 ± 0.005^a	-
AuNPs/SPE	3.99 ± 0.01^b	IR lamp
CNCs/SPE	5.71 ± 0.25^c	IR lamp
AuNPs-CNCs/SPE	7.22 ± 0.17^d	IR lamp

a-d :Means having different letter within each row denote significant difference at $p<0.05$
Data are mean values ± S.D. (n=3)

5.3.3. Effect of pH

The effect of the pH value on the electrochemical behavior of 2,4-TDA was investigated by CV at the AuNPs-CNCs/SPE surface at different pH values ranging from 4 to 10 in a 0.1 M B-R buffer solution containing 500 μM 2,4-TDA. As shown in the Figure 5.3, the oxidation of 2,4-TDA at the AuNPs-CNCs/SPE surface was dramatically affected by the pH of the electrolyte solution. The sensitivity of the electrode for the detection of 2,4-TDA reached its maximum at pH 7.0 which is then used for the following electrochemical measurements.

Furthermore, the oxidation peak potential (E_{pa}) showed a linear decline with increasing pH, indicating that protons were involved in the oxidation reaction of 2,4-TDA. This was further demonstrated by the linear relationship between the pH and oxidation peak potential and expressed as E_{pa}= -26.28pH + 261.26 (R^2= 0.9823). The potential negatively shifted by 26.28 mV per pH unit. As mentioned in the previous chapters, based on the Nernst equation, a slope of 0.0592/2 indicates a proton-to-electron ratio of 2:1, implying that one proton for every two electrons was engaged in the electrochemical oxidation of 2,4-TDA.

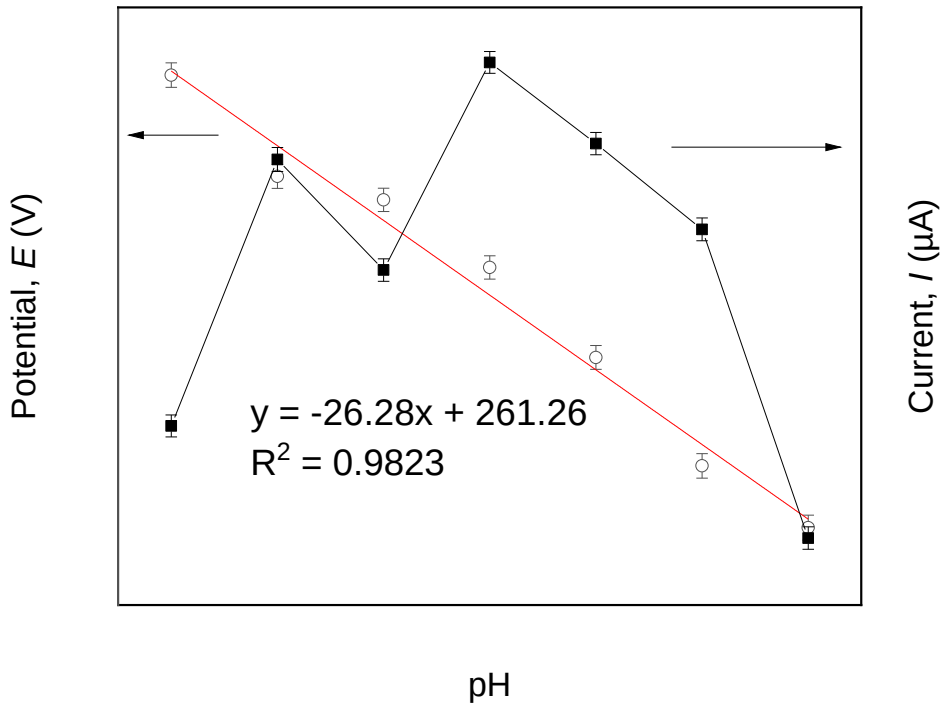

Figure 5.3. Effect of pH value on oxidation peak current and potential of 2,4-TDA (500 μM) at AuNPs-CNCs/SPE

5.3.4. Influence of scan rate

The influence of the scan rate on the electrocatalytic oxidation of 2,4-TDA at the AuNPs-CNCs/SP electrode surface was studied using cyclic voltammetry within the 200–800 mVs^{-1} range (analyte concentration of 500 μM (Figure 5.4). The oxidation peak current (I_p) obtained from each scan rate setting was then plotted against the square root of the scan rate which is shown in the inset of Figure 5.4. The linearity of this plot suggested that the catalytic reaction on the surface of the modified electrode is diffusion-limited.

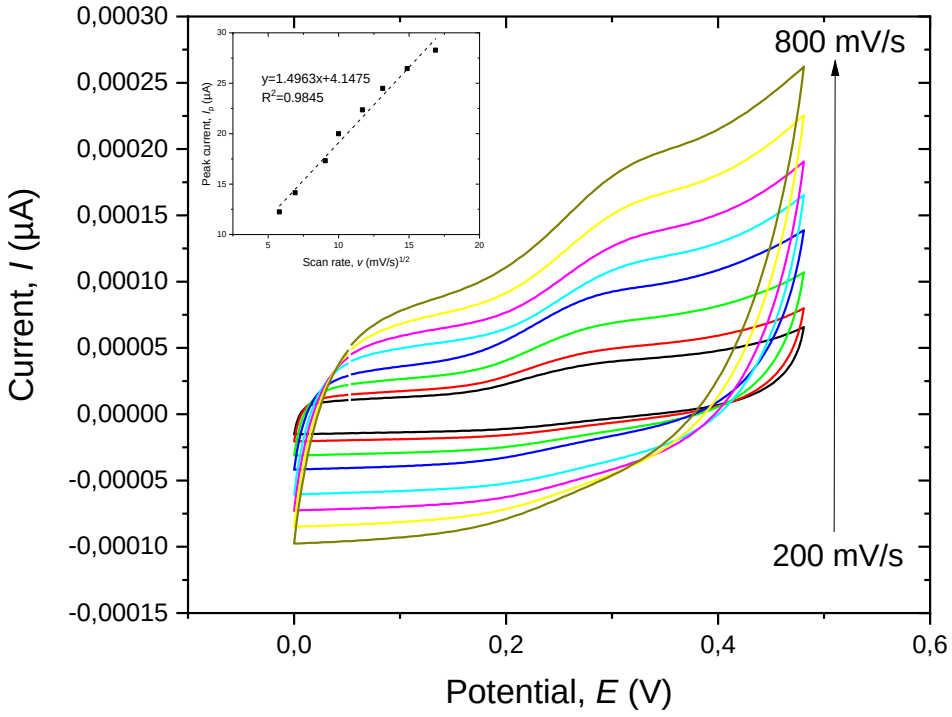

Figure 5.4. Cyclic voltammograms of AuNPs-CNCs/SPE in B-R buffer (pH 7.0) containing 500µM 2,4-TDA at different scan rates (200-800 mVs^{-1}). Inset shows anodic peak current vs. $v^{1/2}$

In order to calculate total number of electrons taking part in the reaction Laviron's theory was applied. Therefore, for a totally irreversible electrode process, the anodic peak potential (E_{pa}) and the natural logarithm of the sacn rate [ln (v)] can be defined by the equation 4.2 stated in section (4.3.4) in Chapter 4. Using the raw voltammogram reported in Figure 5.5 a linear relationship between E_{pa} and ln (v) was obtained as expressed by the equation E_p (v)= 0.0229 ln v + 0.1635.

According to Laviron's equation, electron transfer number (n) can be calculated from the slope of E_{pa} and ln (v), that is, RT/αnF. Finally, n = 2.038~2 was obtained, which suggests that the electrochemical oxidation of 2,4-TDA at the AuNPs-CNCs/SPE surface is a two-electron transfer process.

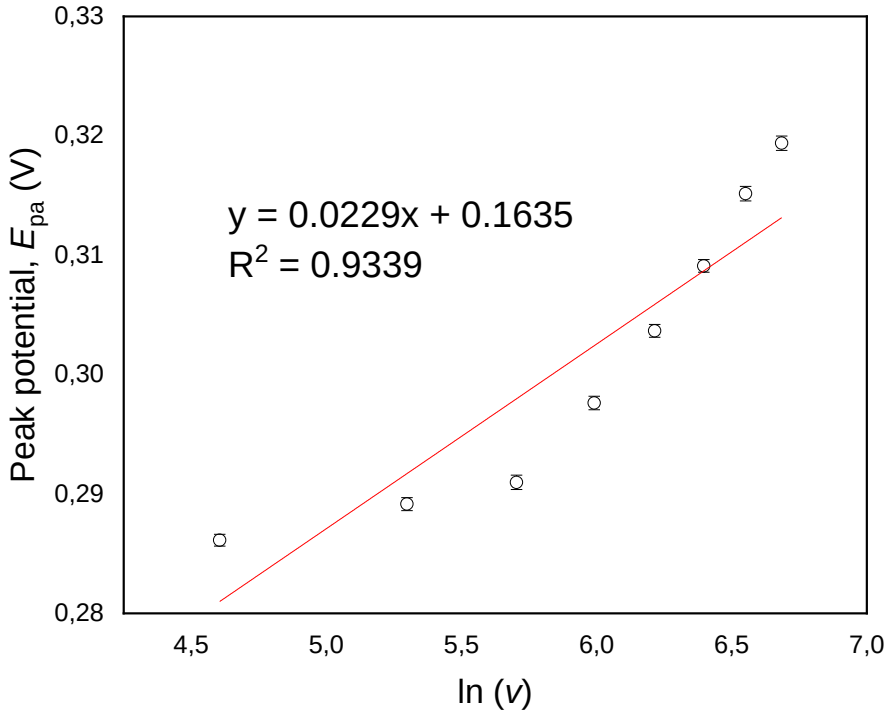

Figure 5.5. The relationship between the peak potential (E_p) and the natural logarithm of scan rates (ln v) for 2,4-TDA (200-800 mVs^{-1})

5.3.5. Chronoamperometric measurements

The electrochemical oxidation of 2,4-TDA at the surface of AuNPs-CNCs/SPE was investigated through chronoamperometry at the potential of 550 mV at different 2,4-TDA concentrations ranging from 0.01 mM to 5 mM in B-R buffer (Figure 5.6).

Cottrell's equation (Eq. 5.2) describes the current response (I) for diffusion-limited electrocatalytic processes of electroactive materials having diffusion coefficient, D.

$$I = \frac{nFAD^{1/2}C_b}{\pi^{1/2}t^{1/2}} \quad (5.2)$$

where n is the number of electrons (2) exchanged per reactant molecule, F is the Faraday constant (9.648×10^4 C mol^{-1}), A is the electrode effective area of the electrode (0.181 cm^2), t is the observation time (s), C_b is the bulk concentration of the analyte (mol cm^{-3}), and D (cm^2 s^{-1}) is the diffusion coefficient of the target analyte (2,4-TDA).

From the raw chronoamperometric traces, a linear curve was obtained for the different concentrations of 2,4 TDA by plotting I against $t^{-1/2}$ (Figure 5.6, inset a). By plotting the slope of each individual straight line, the overall slope of the best-fit line (Figure 5.6, inset b) can be defined from (Eq. 5.3) as:

$$It^{1/2} = \frac{nFAD^{1/2}C_b}{\pi^{1/2}} \tag{5.3}$$

D can thus be drawn from Eq. (5.4)

$$D = \frac{slope^2\pi}{(nFAC_b)^2} \tag{5.4}$$

The overall slope was used within the Cotrell equation to eventually obtain a diffusion coefficient of 1.08×10^{-4} cm^2s^{-1}.

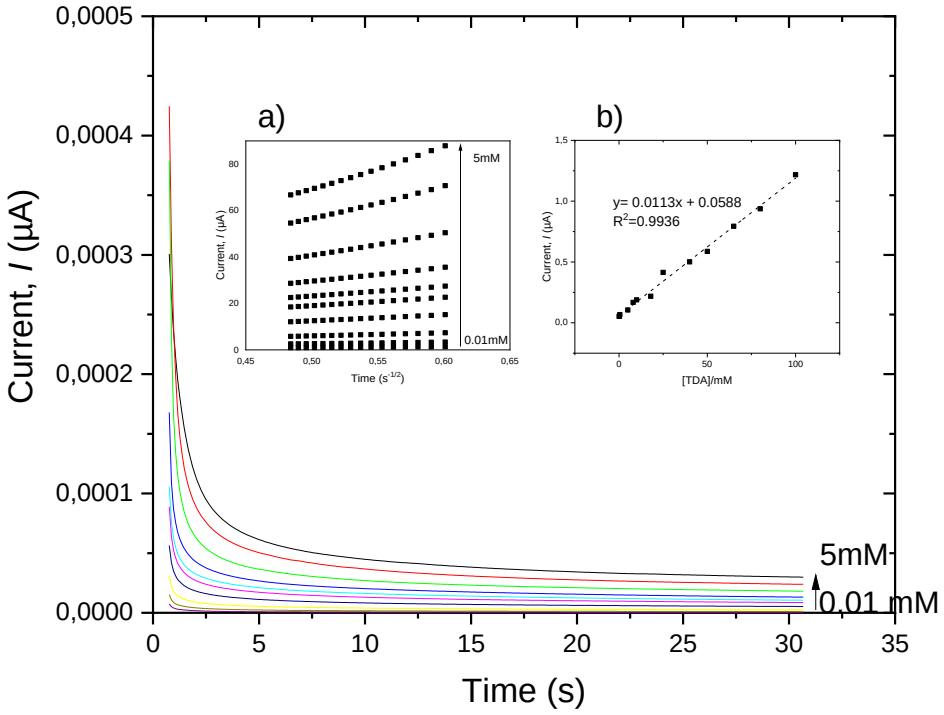

Figure 5.6. Chronoamperograms obtained at AuNPs- CNCs/SPE in B-R buffer (pH 7.0) for different concentrations of 2,4-TDA (0.01-5 mM) of 2,4-TDA. Insets: (a) Plot of I vs. $t^{-1/2}$ obtained from the chronoamperograms (b) Plot of the slope of the straight lines against 2,4-TDA concentration

5.3.6. Differential pulse voltammetric studies

The sensitivity of the AuNPs-CNCs screen-printed electrode to 2,4-TDA was evaluated by differential pulse voltammetry (DPV). In order to achieve the DP voltammograms of 2,4-TDA, proper volumes of the stock solutions of 2,4-TDA were added to the cell containing B-R buffer (9 mL) on total bulk of 10 ml. The voltammetric response of 2,4 TDA at different concentrations in 10 ml Britton-Robinson (B-R) buffer was shown in Figure 5.7. The calibration plot of 2,4-TDA was linear in one concentration range (0.10-120 μM) (Figure 5.8). The sensitivity of the screen-printed modified electrode to 2,4-TDA, calculated as the slope of the linear range in the voltammetric plot, was 0.00104 $\mu A(\mu M)^{-1}$, from which the lower limit of detection (LOD) was calculated according to the following equation (Eq. 5.5):

$$LOD = \frac{3S_{bl}}{m} \quad (5.5)$$

where S_{bl} is the standard deviation (μA) obtained from 10 replicates of the blank solution and m is the slope of the aforementioned linear range in the voltammetric plot. The final LOD value of 0.032 μM was eventually calculated for the AuNPs-CNCs/SP electrode.

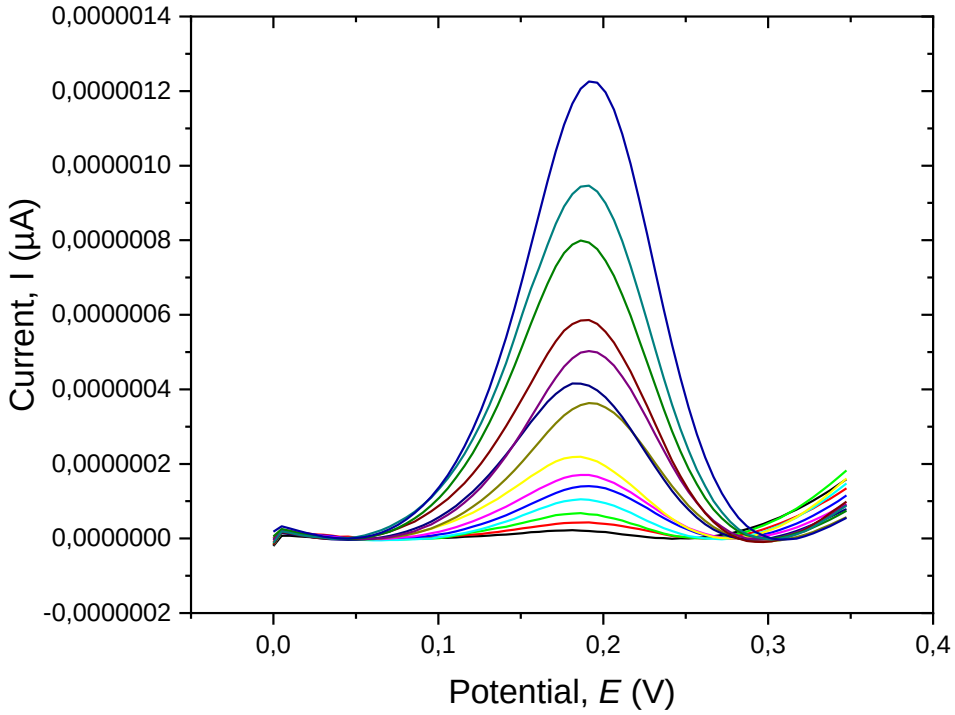

Figure 5.7. Differential pulse voltammetry response of AuNPs-CNCs/SPE in 10 ml B-R buffer (pH 7.0) containing different concentration of 2,4-TDA

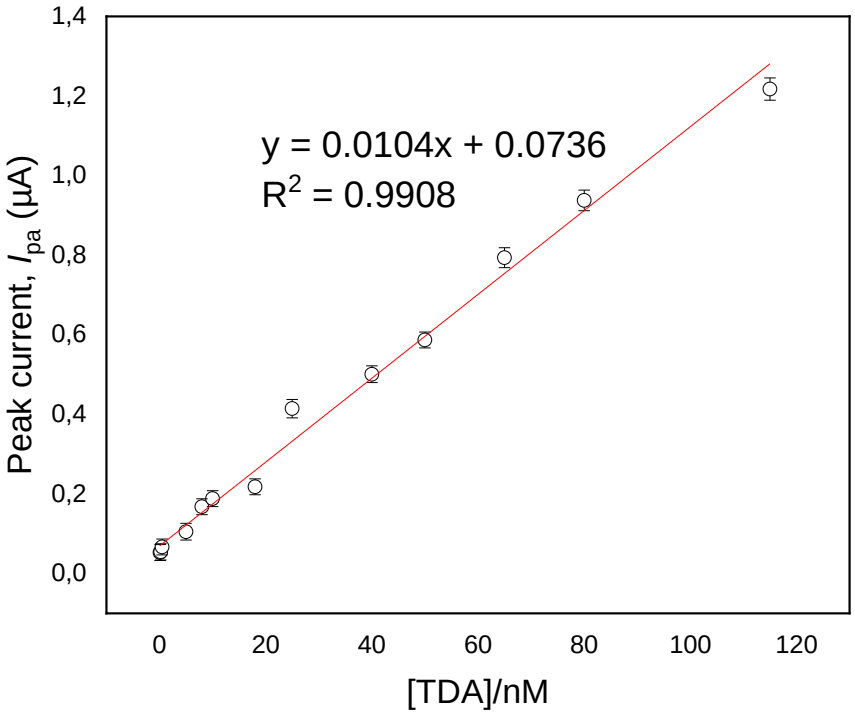

Figure 5.8. 2,4 TDA concentrations ([TDA]/mM) vs. peak current (I_{pa})

5.3.7. Potential interference of other compounds

One of the main problems in real systems is the impairing of functionality in terms of sensor selectivity due to the interference effect of electroactive species other than the target analyte. In PU-based multilayer packaging materials, other primary aromatic amines, and additives commonly used in the manufacturing process are the potential interfering compounds.

In this work, the anti-interference of the modified screen-printed electrode was investigated against two different additives (Irganox® 1010 and Irgafos® 168) that are used during the processing. There was no increase in the current response in the differential pulse voltammetry experiment when the abovementioned compounds were added to the 2,4-TDA containing solution. It can be concluded that the developed sensor can detect and quantify 2,4-TDA selectively.

Finally, the sensor's high repeatability was demonstrated by a relative standard deviation (RSD) of 3.78 % obtained from a single modified electrode (AuNPs-CNCs/SPE) used for five consecutive measurements in the same 2,4-TDA solution (10

μM). In addition, the reproducibility of the proposed sensor was investigated using differential pulse voltammograms at 10 μM 2,4-TDA with five different sensors (AuNPs-CNCs/SPE). The measured RSD (3.35 %) confirms the satisfactory reproducibility of the fabricated sensor.

5.3.8. Real sample analysis

The suitability of the AuNPs-CNCs/SPE as an analytical device for 2,4-TDA determination in real samples was tested by performing a migration test under typical sterilization conditions (121 °C for 20 minutes). For this purpose, food simulant B (3 w/v % acetic acid water solution) was employed within a thermo-sealed pouch, which was subsequently subjected to 121 °C for 20 minutes (sterilization conditions). The conventional addition model was used to evaluate the modified electrode's ability to detect TDA.

As can be seen in Table 5.1, the AuNPs-CNCs-modified electrode worked efficiently, with high recovery (97.88–106.04 %). This result indicates that the AuNPs-CNCs/SPE can be used to detect 2,4-TDA migration from multilayer packages that have been exposed to thermal stresses like sterilization, pasteurization, microwaving, and sous-vide cooking.

Table 5.2. Recovery determination of 2,4-TDA in a food simulant B sample using AuNPs-CNCs/SPE

Sample	Spiked (μM)	Found (μM)	Recovery (%)
Laminate structure (PET/EVOH/PE) including a PU adhesive	0	0	-
	8	7.83	97.88
	25	26.51	106.04
	60	59.07	98.45

5.4. Conclusion

In this work, a new screen-printed electrochemical sensor with high sensitivity and a low limit of detection was developed for the quantification of 2,4-TDA, which is one of the most representative PAAs. As mentioned in the previous chapters, synergistic effect of AuNPs and CNCs was critical in increasing performance of the sensor. The best sensitivity of the electrode for 2,4-TDA was achieved at neutral pH, with an ultimate detection limit of 32 nM. Finally, real sample analysis indicated that the AuNPs-CNCs modified sensor allows reliable quantification of 2,4-TDA and can be considered as an effective alternative to the most prevalent analytical techniques that are used in the detection of primary aromatic amines.

REFERENCES

Anukiruthika, T., Priyanka Sethupathy, Anila Wilson, Kiran Kashampur, Jeyan Arthur Moses, and Chinnaswamy Anandharamakrishnan. "Multilayer packaging: Advances in preparation techniques and emerging food applications." *Comprehensive Reviews in Food Science and Food Safety* 19, no. 3 (2020): 1156-1186. https://doi.org/10.1111/1541-4337.12556.

Arvanitoyannis, Ioannis S., and Loulouda Bosnea. "Migration of substances from food packaging materials to foods." *Critical reviews in food science and nutrition* 44, no. 2 (2004): 63-76. https://doi.org/10.1080/10408690490424621.

Aznar, Margarita, Elena Canellas, and Cristina Nerín. "Quantitative determination of 22 primary aromatic amines by cation-exchange solid-phase extraction and liquid chromatography–mass spectrometry." *Journal of Chromatography A* 1216, no. 27 (2009): 5176-5181. https://doi.org/10.1016/j.chroma.2009.04.096.

Bard, Allen J., Larry R. Faulkner, and Henry S. White. *Electrochemical methods: fundamentals and applications*. John Wiley & Sons, 2022.

Bard, Allen J., György Inzelt, and Fritz Scholz, eds. *Electrochemical dictionary*. Berlin, Heidelberg: Springer Berlin Heidelberg, 2012.

Bard, Allen J., Larry R. Faulkner, and Henry S. White. *Electrochemical methods: fundamentals and applications*. John Wiley & Sons, 2022.

Bijad, Majede, Hassan Karimi-Maleh, and Mohammad A. Khalilzadeh. "Application of ZnO/CNTs nanocomposite ionic liquid paste electrode as a sensitive voltammetric sensor for determination of ascorbic acid in food samples." *Food Analytical Methods* 6, no. 6 (2013): 1639-1647. https://doi.org/10.1007/s12161-013-9585-9.

Brauer, B., and T. Funke. "Determining primary aromatic-amines in migratory solutions." *Deutsche Lebensmittel-Rundschau* 87, no. 9 (1991): 280-281.

Brede*, C., and I. Skjevrak. "Migration of aniline from polyamide cooking utensils into food simulants." *Food additives and contaminants* 21, no. 11 (2004): 1115-1124.

Brede, Cato, Ingun Skjevrak, and Hallgeir Herikstad. "Determination of primary aromatic amines in water food simulant using solid-phase analytical derivatization followed by gas chromatography coupled with mass spectrometry." *Journal of Chromatography A* 983, no. 1-2 (2003): 35-42.

Butler, Thomas I., and Barry A. Morris. "PE-based multilayer film structures." In *Multilayer flexible packaging*, pp. 281-310. William Andrew Publishing, 2016.

Butwong, Nutthaya, Jariya Khajonklin, Atitaya Thongbor, and John HT Luong. "Electrochemical sensing of histamine using a glassy carbon electrode modified with multiwalled carbon nanotubes decorated with Ag-Ag_2O nanoparticles." *Microchimica Acta* 186, no. 11 (2019): 1-10. https://doi.org/10.1007/s00604-019-3860-4

Büyüktaş, Duygu, Masoud Ghaani, Cesare Rovera, Richard T. Olsson, Figen Korel, and Stefano Farris. "Development of a nano-modified glassy carbon electrode for the determination of 2, 6-diaminotoluene (TDA)." *Food Packaging and Shelf Life* 29 (2021): 100714. https://doi.org/10.1016/j.fpsl.2021.100714

Cai, Guohui, Kun Ge, Xiaoyan Ouyang, Yuling Hu, and Gongke Li. "Thin-layer chromatography combined with surface-enhanced Raman scattering for rapid detection of benzidine and 4-aminobiphenyl in migration from food contact materials based on gold nanoparticle doped metal-organic framework." *Journal of Separation Science* 43, no. 14 (2020): 2834-2841. https://doi.org/10.1002/jssc.202000145

Campanella, Gaetano, Masoud Ghaani, Gianpiero Quetti, and Stefano Farris. "On the origin of primary aromatic amines in food packaging materials." *Trends in Food Science & Technology* 46, no. 1 (2015): 137-143. https://doi.org/10.1016/j.tifs.2015.09.002

Chen, Ningning, Li Chen, Yuxiao Cheng, Kai Zhao, Xiaohong Wu, and Yuezhong Xian. "Molecularly imprinted polymer grafted graphene for simultaneous electrochemical sensing of 4, 4-methylene diphenylamine and aniline by differential pulse voltammetry." *Talanta* 132 (2015): 155-161. https://doi.org/10.1016/j.talanta.2014.09.008.

Dadkhah, Sahar, Ehsan Ziaei, Ali Mehdinia, Tohid Baradaran Kayyal, and Ali Jabbari. "A glassy carbon electrode modified with amino-functionalized graphene oxide and molecularly imprinted polymer for electrochemical sensing of bisphenol A." *Microchimica Acta* 183, no. 6 (2016): 1933-1941. https://doi.org/10.1007/s00604-016-1824-5.

Daizy, Mahbuba, Chaitaly Tarafder, Md Rashid Al-Mamun, Xiuhua Liu, Mohamed Aly Saad Aly, and Md Zaved H. Khan. "Electrochemical detection of melamine by using reduced graphene oxide–copper nanoflowers modified glassy carbon electrode." *ACS omega* 4, no. 23 (2019): 20324-20329. https://doi.org/10.1021/acsomega.9b02827.

de Fátima Pocas, Maria, and Timothy Hogg. "Exposure assessment of chemicals from packaging materials in foods: a review." *Trends in Food Science & Technology* 18, no. 4 (2007): 219-230. https://doi.org/10.1016/j.tifs.2006.12.008.

Deng, Peihong, Zhifeng Xu, and Yunfei Kuang. "Electrochemical determination of bisphenol A in plastic bottled drinking water and canned beverages using a molecularly imprinted chitosan–graphene composite film modified electrode." *Food chemistry* 157 (2014): 490-497.Dixon, J (2011). Multilayer packaging for food and beverages. *Packaging materials*, Europe: ILSI. https://doi.org/10.1016/j.foodchem.2014.02.074.

Dorovskikh, Svetlana I., Darya D. Klyamer, Anastasiya D. Fedorenko, Natalia B. Morozova, and Tamara V. Basova. "Electrochemical Sensor Based on Iron (II) Phthalocyanine and Gold Nanoparticles for Nitrite Detection in Meat Products." *Sensors* 22, no. 15 (2022): 5780. https://doi.org/10.3390/s22155780.

Ellendt, K., B. Gutsche, and G. Steiner. "Analysis of laminates-Determination of isocyanate residues and primary aromatic amine migration." *Deutsche Lebensmittel-Rundschau* 99, no. 4 (2003): 131-136.

Emambakhsh, Fatemeh, Hamideh Asadollahzadeh, Nahid Rastakhiz, and Sayed Zia Mohammadi. "Highly sensitive determination of Bisphenol A in water and milk samples by using magnetic activated carbon–Cobalt nanocomposite-screen printed electrode." *Microchemical Journal* 179 (2022): 107466. https://doi.org/10.1016/j.microc.2022.107466.

EC. "Commission Regulation (EC) No 2023/2006 of 22 December 2006 on good manufacturing practice for materials and articles intended to come into contact with food." *Off J Eur Union.* 50 (2006): 75-78.

EC (European Commission). "Commission Regulation (EU) No 10/2011 of 14 January 2011 on plastic materials and articles intended to come contact with food." (2011).

Fakhari, Ali Reza, Hamid Ahmar, Hadi Hosseini, and Siyavash Kazemi Movahed. "Fabrication of novel redox-active poly (4, 5-dihydro-1, 3-thiazol-2-ylsulfanyl-3-methyl-1, 2-benzenediol)-gold nanoparticles film on MWCNTs modified electrode: application as the electrochemical sensor for the determination of hydrazine." *Sensors and Actuators B: Chemical* 213 (2015): 82-91. https://doi.org/10.1016/j.snb.2015.02.015

Feizollahi, Azizallah, Amir Abbas Rafati, Parnaz Assari, and Roghayeh Asadpour Joghani. "Development of an electrochemical sensor for the determination of antibiotic sulfamethazine in cow milk using graphene oxide decorated with Cu–Ag core–shell nanoparticles." *Analytical Methods* 13, no. 7 (2021): 910-917. https://doi.org/10.1039/D0AY02261F.

Fu, Caili, Chang Liu, Ying Li, Yajing Guo, Fang Luo, Peilong Wang, Longhua Guo, Bin Qiu, and Zhenyu Lin. "Homogeneous electrochemical biosensor for melamine based on DNA triplex structure and exonuclease III-assisted recycling amplification." *Analytical chemistry* 88, no. 20 (2016): 10176-10182. https://doi.org/10.1021/acs.analchem.6b02753.

Ghaani, Masoud, Carlo A. Cozzolino, Giulia Castelli, and Stefano Farris. "An overview of the intelligent packaging technologies in the food sector." *Trends in Food Science & Technology* 51 (2016): 1-11. https://doi.org/10.1016/j.tifs.2016.02.008.

Ghaani, Masoud, Flavia Pucillo, Richard T. Olsson, Matteo Scampicchio, and Stefano Farris. "A bionanocomposite-modified glassy carbon electrode for the determination of 4, 4′-methylene diphenyl diamine." *Analytical Methods* 10, no. 34 (2018a): 4122-4128. https://doi.org/ 10.1039/c8ay01376d.

Ghaani, Masoud, Cesare Rovera, Flavia Pucillo, Mohammad R. Ghaani, Richard T. Olsson, Matteo Scampicchio, and Stefano Farris. "Determination of 2, 4-diaminotoluene by a bionanocomposite modified glassy carbon electrode." *Sensors and Actuators B: Chemical* 277 (2018b): 477-483. https://doi.org/10.1016/j.snb.2018.09.053.

Gheibi, Siamak, Hassan Karimi-Maleh, Mohammad A. Khalilzadeh, and Hasan Bagheri. "A new voltammetric sensor for electrocatalytic determination of vitamin C in fruit juices and fresh vegetable juice using modified multi-wall carbon nanotubes paste electrode." *Journal of Food Science and Technology* 52, no. 1 (2015): 276-284. https://doi.org/10.1007/s13197-013-1026-7.

Goulas, Antonios E., Kyriakos A. Riganakos, and Michael G. Kontominas. "Effect of ionizing radiation on physicochemical and mechanical properties of commercial multilayer coextruded flexible plastics packaging materials." *Radiation Physics and Chemistry* 68, no. 5 (2003): 865-872. https://doi.org/10.1016/S0969-806X(03)00298-6

Jiao, Shoufeng, Jing Jin, and Lun Wang. "One-pot preparation of Au-RGO/PDDA nanocomposites and their application for nitrite sensing." *Sensors and Actuators B: Chemical* 208 (2015): 36-42. https://doi.org/10.1016/j.snb.2014.11.020.

Jin, Guiying, Yuzhong Zhang, and Wangxing Cheng. "Poly (p-aminobenzene sulfonic acid)-modified glassy carbon electrode for simultaneous detection of dopamine and ascorbic acid." *Sensors and Actuators B: Chemical* 107, no. 2 (2005): 528-534. https://doi.org/10.1016/j.snb.2004.11.018.

Hanssen, Benjamin L., Shajahan Siraj, and Danny KY Wong. "Recent strategies to minimise fouling in electrochemical detection systems." *Reviews in Analytical Chemistry* 35, no. 1 (2016): 1-28. https://doi.org/10.1515/revac-2015-0008

Huang, De-Qian, Cheng Chen, Yi-Ming Wu, Hong Zhang, Liang-Quan Sheng, Hua-Jie Xu, and Zhao-Di Liu. "The determination of dopamine using glassy carbon electrode pretreated by a simple electrochemical method." *Int. J. Electrochem. Sci* 7 (2012): 5510-5520.

Huang, Jiadong, Xiuming Zhang, Qing Lin, Xiaorui He, Xianrong Xing, Hongxia Huai, Wenjing Lian, and Han Zhu. "Electrochemical sensor based on imprinted sol–gel and nanomaterials for sensitive determination of bisphenol A." *Food Control* 22, no. 5 (2011): 786-791. https://doi.org/10.1016/j.foodcont.2010.11.017.

Kadara, Rashid O., Barry GD Haggett, and Brian J. Birch. "Disposable sensor for measurement of vitamin B2 in nutritional premix, cereal, and milk powder." *Journal of agricultural and food chemistry* 54, no. 14 (2006): 4921-4924. https://doi.org/10.1021/jf0603376.

Kaiser, Katharina, Markus Schmid, and Martin Schlummer. "Recycling of polymer-based multilayer packaging: A review." *Recycling* 3, no. 1 (2017): 1. https://doi.org/10.3390/recycling3010001.

Khanna, Mansi, Souradeep Roy, Ranjit Kumar, Shikha Wadhwa, Ashish Mathur, and Ashwani Kumar Dubey. "MnO 2 based bisphenol-A electrochemical sensor using micro-fluidic platform." *IEEE Sensors Journal* 18, no. 6 (2018): 2206-2210. https//:doi.org/10.1109/jsen.2018.2792476.

Knežević, Sara, Miloš Ognjanović, Nemanja Nedić, Jose FML Mariano, Zorana Milanović, Branka Petković, Bratislav Antić, Sanja Vranješ Djurić, and Dalibor Stanković. "A single drop histamine sensor based on AuNPs/MnO2 modified screen-printed electrode." *Microchemical Journal* 155 (2020): 104778. https://doi.org/10.1016/j.microc.2020.104778.

Kouhi, Iraj, Golnaz Parvizi Fard, Esmaeel Alipour, and Afsaneh Saadatirad. "Development of an electrochemical sensor for determination of vanillin in

some food stuffs." *Journal of Food Processing and Preservation* 46, no. 2 (2022): e16289. https://doi.org/10.1111/jfpp.16289.

Lambertini, Francesca, Valentina Di Lallo, Dante Catellani, Monica Mattarozzi, Maria Careri, and Michele Suman. "Reliable liquid chromatography-mass spectrometry method for investigation of primary aromatic amines migration from food packaging and during industrial curing of multilayer plastic laminates." *Journal of Mass Spectrometry* 49, no. 9 (2014): 870-877. https://doi.org/10.1002/jms.3436.

Lapprand, Aude, Fernande Boisson, Frédéric Delolme, Françoise Méchin, and J-P. Pascault. "Reactivity of isocyanates with urethanes: Conditions for allophanate formation." *Polymer degradation and stability* 90, no. 2 (2005): 363-373. https://doi.org/10.1016/j.polymdegradstab.2005.01.045.

Laviron, E. "Adsorption, autoinhibition and autocatalysis in polarography and in linear potential sweep voltammetry." *Journal of Electroanalytical Chemistry and Interfacial Electrochemistry* 52, no. 3 (1974): 355-393. https://doi.org/10.1016/S0022-0728(74)80448-1.

Lee, Dong Sun, Kit L. Yam, and Luciano Piergiovanni. *Food packaging science and technology*. CRC press, 2008. https://doi.org/10.1201/9781439894071.

Li, Xiangjun, Xiaojiao Wang, Leilei Li, Huimin Duan, and Chuannan Luo. "Electrochemical sensor based on magnetic graphene oxide@ gold nanoparticles-molecular imprinted polymers for determination of dibutyl phthalate." *Talanta* 131 (2015): 354-360. https://doi.org/10.1016/j.talanta.2014.07.028.

Long, Fang, Zhaohui Zhang, Jing Wang, Liang Yan, and Biwu Zhou. "Cobalt-nickel bimetallic nanoparticles decorated graphene sensitized imprinted electrochemical sensor for determination of octylphenol." *Electrochimica Acta* 168 (2015): 337-345. https://doi.org/10.1016/j.electacta.2015.04.054.

Lounasvuori, Mailis M., David Kelly, and John S. Foord. "Carbon black as low-cost alternative for electrochemical sensing of phenolic compounds." *Carbon* 129 (2018): 252-257. https://doi.org/10.1016/j.carbon.2017.12.020.

Malucelli, Giulio, Aldo Priola, Franco Ferrero, Andrea Quaglia, Mariaenrica Frigione, and Cosimo Carfagna. "Polyurethane resin-based adhesives: curing reaction and properties of cured systems." *International Journal of Adhesion and Adhesives* 25, no. 1 (2005): 87-91. https://doi.org/10.1016/j.ijadhadh.2004.04.003.

Mariyappan, Vinitha, Naveen Karuppusamy, Shen-Ming Chen, Paulsamy Raja, and Rasu Ramachandran. "Electrochemical determination of quercetin using glassy carbon electrode modified with WS2/GdCoO3 nanocomposite." *Microchimica Acta* 189, no. 3 (2022): 1-14. https://doi.org/10.1007/s00604-022-05219-3.

Masawat, Prinya, and Jonathan Mark Slater. "The determination of tetracycline residues in food using a disposable screen-printed gold electrode (SPGE)." *Sensors and Actuators B: Chemical* 124, no. 1 (2007): 127-132. https://doi.org/10.1016/j.snb.2006.12.010.

Mattarozzi, Monica, Francesca Lambertini, Michele Suman, and Maria Careri. "Liquid chromatography–full scan-high resolution mass spectrometry-based method towards the comprehensive analysis of migration of primary aromatic amines from food packaging." *Journal of Chromatography A* 1320 (2013): 96-102. https://doi.org/10.1016/j. chroma.2013.10.063.

Meier-Westhues, Ulrich, K. Danielmeier, P. Kruppa, and E. Squiller. "Polyurethanes: Coatings." *Adhesives and Sealants* (2007): 45-46.

Metters, Jonathan P., Rashid O. Kadara, and Craig E. Banks. "New directions in screen printed electroanalytical sensors: an overview of recent developments." *Analyst* 136, no. 6 (2011): 1067-1076. https://doi.org/10.1039/C0AN00894J.

Moreno, Mónica, Alberto Sánchez Arribas, Esperanza Bermejo, Manuel Chicharro, Antonio Zapardiel, Marcela C. Rodríguez, Yamile Jalit, and Gustavo A. Rivas. "Selective detection of dopamine in the presence of ascorbic acid using carbon nanotube modified screen-printed electrodes." *Talanta* 80, no. 5 (2010): 2149-2156. https://doi.org/10.1016/j.talanta.2009.11.022.

Morris, Barry A. *The science and technology of flexible packaging: multilayer films from resin and process to end use*. William Andrew, 2022.

Mortensen, Sarah Kelly, Xenia Thorsager Trier, Annie Foverskov, and Jens Højslev Petersen. "Specific determination of 20 primary aromatic amines in aqueous food simulants by liquid chromatography–electrospray ionization-tandem mass spectrometry." *Journal of Chromatography A* 1091, no. 1-2 (2005): 40-50. https://doi.org/10.1016/j.chroma.2005.07.026.

Mukhopadhyay, Subhas Chandra, ed. *Next generation sensors and systems*. Vol. 16. Cham: Springer International Publishing, 2016.

Nasiri, Hasan, Hamed Baghban, Reza Teimuri-Mofrad, and Ahad Mokhtarzadeh. "Graphitic carbon nitride/magnetic chitosan composite for rapid electrochemical detection of lactose." *International Dairy Journal* 136 (2023): 105489.

Nasirizadeh, Navid, Zahra Shekari, and Masoud Ghaani. "A novel electrochemical biosensor based on a modified gold electrode for hydrogen peroxide determination in different beverage samples." *Food Analytical Methods* 8, no. 6 (2015): 1546-1555. https://doi.org/10.1007/s10008-010-1259-6.

Nasirizadeh, Navid, Zahra Shekari, Hamid R. Zare, and Somayeh Makarem. "Electrocatalytic determination of dopamine in the presence of uric acid using an indenedione derivative and multiwall carbon nanotubes spiked in carbon paste electrode." *Materials Science and Engineering: C* 33, no. 3 (2013): 1491-1497. https://doi.org/10.1016/j.msec.2012.12.051.

Nasirizadeh, Navid, Masoud Ghaani, Zahra Shekari, and Mohammad Shateri-Khalilabad. "Novel non enzymatic TBHQ modified electrochemical sensor for hydrogen peroxide determination in different beverage samples." *Journal of the Brazilian Chemical Society* 27 (2016): 1577-1586. https://doi.org/10.5935/0103-5053.20160037

Pezo, Davinson, Mauro Fedeli, Osvaldo Bosetti, and Cristina Nerín. "Aromatic amines from polyurethane adhesives in food packaging: The challenge of identification and pattern recognition using Quadrupole-Time of Flight-Mass SpectrometryE." *Analytica chimica acta* 756 (2012): 49-59. https://doi.org/10.1016/j.aca.2012.10.031

Rahman, Mohammed M., and Jahir Ahmed. "Cd-doped Sb2O4 nanostructures modified glassy carbon electrode for efficient detection of melamine by electrochemical approach." *Biosensors and Bioelectronics* 102 (2018): 631-636. https://doi.org/10.1016/j.bios.2017.12.007

Rassaei, Liza, Frank Marken, Mika Sillanpää, Mandana Amiri, Ciprian Mihai Cirtiu, and Markus Sillanpää. "Nanoparticles in electrochemical sensors for environmental monitoring." *TrAC Trends in Analytical Chemistry* 30, no. 11 (2011): 1704-1715. https://doi.org/10.1016/j.trac.2011.05.009

Rehman, Abdul, Naseer Iqbal, Peter A. Lieberzeit, and Franz L. Dickert. "Multisensor biomimetic systems with fully artificial recognition strategies in food analysis." *Monatshefte für Chemie-Chemical Monthly* 140, no. 8 (2009): 931-939. https://doi.org/10.1007/s00706-009-0151-5.

Renedo, O. Dominguez, M. A. Alonso-Lomillo, and MJ Arcos Martínez. "Recent developments in the field of screen-printed electrodes and their related applications." *Talanta* 73, no. 2 (2007): 202-219. https://doi.org/10.1016/j.talanta.2007.03.050.

Rollini, Manuela, Alida Musatti, Daniele Cavicchioli, Daniele Bussini, Stefano Farris, Cesare Rovera, Diego Romano, Stefano De Benedetti, and Alberto Barbiroli. "From cheese whey permeate to Sakacin-A/bacterial cellulose nanocrystal conjugates for antimicrobial food packaging applications: a circular economy case study." *Scientific Reports* 10, no. 1 (2020): 1-14. https://doi.org/10.1038/s41598-020-78430-y.

Rosato, Dominick V. *Extruding plastics: a practical processing handbook*. Springer Science & Business Media, 2013.

Rovera, Cesare, Masoud Ghaani, Nadia Santo, Silvia Trabattoni, Richard T. Olsson, Diego Romano, and Stefano Farris. "Enzymatic hydrolysis in the green production of bacterial cellulose nanocrystals." *ACS Sustainable Chemistry & Engineering* 6, no. 6 (2018): 7725-7734. https://doi.org/10.1021/acssuschemeng.8b00600.

Qaanei, Masood, Ramezan Ali Taheri, and Khadijeh Eskandari. "Electrochemical aptasensor for Escherichia coli O157: H7 bacteria detection using a

nanocomposite of reduced graphene oxide, gold nanoparticles and polyvinyl alcohol." *Analytical Methods* 13, no. 27 (2021): 3101-3109. https://doi.org/10.1039/D1AY00563D.

Salimi, Abdollah, Hussein MamKhezri, and Rahman Hallaj. "Simultaneous determination of ascorbic acid, uric acid and neurotransmitters with a carbon ceramic electrode prepared by sol–gel technique." *Talanta* 70, no. 4 (2006): 823-832. https://doi.org/10.1016/j.talanta.2006.02.015.

Sanchis, Yovana, Vicent Yusà, and Clara Coscollà. "Analytical strategies for organic food packaging contaminants." *Journal of Chromatography A* 1490 (2017): 22-46.

Sanchis, Yovana, Clara Coscollà, and Vicent Yusà. "Comprehensive analysis of photoinitiators and primary aromatic amines in food contact materials using liquid chromatography high-resolution mass spectrometry." *Talanta* 191 (2019): 109-118. https://doi.org/ 10.1016/j.talanta.2018.08.047.

Sendón, Raquel, Juana Bustos, Jose Juan Sánchez, Perfecto Paseiro, and Ma Eugenia Cirugeda. "Validation of a liquid chromatography–mass spectrometry method for determining the migration of primary aromatic amines from cooking utensils and its application to actual samples." *Food Additives and Contaminants* 27, no. 1 (2010): 107-117. https://doi.org/10.1080/ 02652030903225781.

Shrivastava, Alankar, and Vipin B. Gupta. "Methods for the determination of limit of detection and limit of quantitation of the analytical methods." *Chron. Young Sci* 2, no. 1 (2011): 21-25. https://doi.org/10.4103/2229-5186.79345.

Skoog, D. A., F. James Holler, and S. R. Crouch. "Principles of instrumental analysis. thomson brooks." *Cole, Canada* (2007).

Song, Debin, Qiaowei Chen, Chunyang Zhai, Hengcong Tao, Lina Zhang, Tianbo Jia, Zhiwang Lu, Wuyang Sun, Pengxiang Yuan, and Baikang Zhu. "Label-Free ZnIn2S4/UiO-66-NH2 Modified Glassy Carbon Electrode for Electrochemically Assessing Fish Freshness by Monitoring Xanthine and Hypoxanthine." *Chemosensors* 10, no. 5 (2022): 158. https://doi.org/10.3390/chemosensors10050158.

Su, Wan-Yu, Sheng-Ming Wang, and Shu-Hua Cheng. "Electrochemically pretreated screen-printed carbon electrodes for the simultaneous determination of aminophenol isomers." *Journal of Electroanalytical Chemistry* 651, no. 2 (2011): 166-172. https://doi.org/10.1016/j.jelechem.2010.11.028.

Sun, Dong, and Huajie Zhang. "Voltammetric determination of 6-benzylaminopurine (6-BAP) using an acetylene black-dihexadecyl hydrogen phosphate composite film coated glassy carbon electrode." *Analytica chimica acta* 557, no. 1-2 (2006): 64-69. https://doi.org/ 10.1016/j.aca.2005.10.002.

Sun, Wei, Xiaowei Qi, Yuanyuan Zhang, Hairong Yang, Hongwei Gao, Ying Chen, and Zhenfan Sun. "Electrochemical DNA biosensor for the detection of Listeria monocytogenes with dendritic nanogold and electrochemical reduced graphene modified carbon ionic liquid electrode." *Electrochimica Acta* 85 (2012): 145-151. https://doi.org/10.1016/j.electacta.2012.07.133.

Talarico, Daria, Fabiana Arduini, Alessia Constantino, Michele Del Carlo, Dario Compagnone, Danila Moscone, and Giuseppe Palleschi. "Carbon black as successful screen-printed electrode modifier for phenolic compound detection." *Electrochemistry Communications* 60 (2015): 78-82. https://doi.org/10.1016/j.elecom.2015.08.010.

Tefera, Molla, Merid Tessema, Shimelis Admassie, Emmanuel I. Iwuoha, Tesfaye T. Waryo, and Priscilla GL Baker. "Electrochemical determination of phenothrin in fruit juices at graphene oxide-polypyrrole modified glassy carbon electrode." *Sensing and bio-sensing research* 21 (2018): 27-34. https://doi.org/10.1016/j.sbsr.2018.09.003.

Thandavan, Kavitha, Sakthivel Gandhi, Noel Nesakumar, Swaminathan Sethuraman, John Bosco Balaguru Rayappan, and Uma Maheswari Krishnan. "Hydrogen peroxide biosensor utilizing a hybrid nano-interface of iron oxide nanoparticles and carbon nanotubes to assess the quality of milk." *Sensors and Actuators B: Chemical* 215 (2015): 166-173. https://doi.org/10.1016/j.snb.2015.03.041.

Tu, Xinman, Liushui Yan, Xubiao Luo, Shenglian Luo, and Qingji Xie. "Electroanalysis of Bisphenol A at a Multiwalled Carbon Nanotubes-gold Nanoparticles Modified Glassy Carbon Electrode." *Electroanalysis: An*

International Journal Devoted to Fundamental and Practical Aspects of Electroanalysis 21, no. 22 (2009): 2491-2494. https://doi.org/10.1002/elan.200900195.

Turkish Food Codex Plastics in Contact with Food Substrates and Materials Communique, (2019, 25, December). Official Gazette (Issue 30989).

Ubeda, Sara, Margarita Aznar, Anna Kjerstine Rosenmai, Anne Marie Vinggaard, and Cristina Nerín. "Migration studies and toxicity evaluation of cyclic polyesters oligomers from food packaging adhesives." *Food chemistry* 311 (2020): 125918.https://doi.org/10.1016/j. foodchem.2019.125918

U.S. Food and Drugs Administration. Subpart, A. "PART 177—INDIRECT FOOD ADDITIVES: POLYMERS."

Vineis, Paolo, and Roberta Pirastu. "Aromatic amines and cancer." *Cancer Causes & Control* 8, no. 3 (1997): 346-355. https://doi.org/10.1023/A:1018453104303.

Viswanathan, Subramanian, and Jerzy Radecki. "Nanomaterials in electrochemical biosensors for food analysis-a review." *Polish journal of food and nutrition sciences* 58, no. 2 (2008).

Xi, Huiting, Xingguang Chen, Yao Cao, Junjun Xu, Cuizhu Ye, Danwen Deng, Jinsheng Zhang, and Ganhui Huang. "Electrochemical determination of formaldehyde via reduced AuNPs@ PPy composites modified electrode." *Microchemical Journal* 156 (2020): 104846. https://doi.org/10.1016/j.microc.2020.104846.

Wagner Jr, John R., ed. *Multilayer flexible packaging*. William Andrew, 2016.

Wang, J. (2001). Analytical Electrochemistry. New Jersey: John Wiley & Sons.

Wang, Hai-Bo, Hong-Ding Zhang, Lu-Lu Xu, Tian Gan, Ke-Jing Huang, and Yan-Ming Liu. "Electrochemical biosensor for simultaneous determination of guanine and adenine based on dopamine-melanin colloidal nanospheres–graphene composites." *Journal of Solid State Electrochemistry* 18, no. 9 (2014): 2435-2442. https://doi.org/10.1007/s10008-014- 2494-z.

Wang, Hai-Bo, Hong-Ding Zhang, Yue-Hua Zhang, Huan Chen, Lu-Lu Xu, Ke-Jing Huang, and Yan-Ming Liu. "Tungsten disulfide nano-flowers/silver nanoparticles composites based electrochemical sensor for theophylline determination." *Journal of the Electrochemical Society* 162, no. 7 (2015): B173. https://doi.org/10.1149/2.0941507jes.

Wang, P. L., Xu Liu, Q. Q. Hu, Hui Gao, and Wei Ma. "Simple and Rapid Determination of Tartrazine Using Poly (l-arginine)/Electrochemically Reduced Graphene Oxide Modified Glassy Carbon Electrode." *Int. J. Electrochem. Sci* 15, no. 9 (2020): 8901-8912.

Wang, Xiaoyu, and Yi Chen. "Determination of aromatic amines in food products and composite food packaging bags by capillary electrophoresis coupled with transient isotachophoretic stacking." *Journal of Chromatography A* 1216, no. 43 (2009): 7324-7328. https://doi.org/10.1016/j.chroma.2009.05.089.

Wang, Yazhen, Bin Song, Junhui Xu, and Shengshui Hu. "An amperometric sensor for nitric oxide based on a glassy carbon electrode modified with graphene, Nafion, and electrodeposited gold nanoparticles." *Microchimica Acta* 182, no. 3 (2015): 711-718. https://doi.org/10.1007/s00604-014-1379-2

Wang, Yanxin, Liyun Zhang, Dapeng Peng, Shuyu Xie, Dongmei Chen, Yuanhu Pan, Yanfei Tao, and Zonghui Yuan. "Construction of electrochemical immunosensor based on gold-nanoparticles/carbon nanotubes/chitosan for sensitive determination of T-2 toxin in feed and swine meat." *International journal of molecular sciences* 19, no. 12 (2018): 3895. https://doi.org/10.3390/ijms19123895

Yan, J. W., C. Hu, L. H. Tong, Z. X. Lei, and Qin-Bao Lin. "Migration test and safety assessment of polyurethane adhesives used for food-contact laminated films." *Food Packaging and Shelf Life* 23 (2020): 100449. https://doi.org/10.1016/j. fpsl.2019.100449

Yoshitake, Norimichi, and Mutsuhisa Furukawa. "Thermal degradation mechanism of α, γ-diphenyl alkyl allophanate as a model polyurethane by pyrolysis-high-

resolution gas chromatography/FT-IR." *Journal of analytical and applied pyrolysis* 33 (1995): 269-281. https://doi.org/10.1016/0165-2370(94)00840-W.

Yu, Liangyun, Qi Zhang, Bairen Yang, Qi Xu, Qin Xu, and Xiaoya Hu. "Electrochemical sensor construction based on Nafion/calcium lignosulphonate functionalized porous graphene nanocomposite and its application for simultaneous detection of trace Pb2+ and Cd2+." *Sensors and Actuators B: Chemical* 259 (2018): 540-551. https://doi.org/10.1016/j.snb.2017.12.103

Yu, Wenlong, Yaxin Sang, Tianying Wang, Weihua Liu, and Xianghong Wang. "Electrochemical immunosensor based on carboxylated single-walled carbon nanotube-chitosan functional layer for the detection of cephalexin." *Food Science & Nutrition* 8, no. 2 (2020): 1001-1011. https://doi.org/10.1002/fsn3.1382.

Zare, H. R., N. Nasirizadeh, and M. Mazloum Ardakani. "Electrochemical properties of a tetrabromo-p-benzoquinone modified carbon paste electrode. Application to the simultaneous determination of ascorbic acid, dopamine and uric acid." *Journal of Electroanalytical Chemistry* 577, no. 1 (2005): 25-33. https://doi.org/10.1016/j. jelechem.2004.11.010

Zhang, Hongyuan, Dawei Sun, and Tieping Cao. "Electrochemical Sensor Based on Silver Nanoparticles/Multi-walled Carbon Nanotubes Modified Glassy Carbon Electrode to Detect Cyanide in Food Products." *Int. J. Electrochem. Sci* 15 (2020): 3434-3444. http://doi.org/10.20964/2020.04.32

Zhang, Hongding, Zhenhua Xing, Miaomiao Pan, Hai-Bo Wang, and Yan-Ming Liu. "Highly sensitive and selective electrochemical determination of 4-aminophenol based on flower-like Ag-Au nanocomposites modified glassy carbon electrode." *Journal of The Electrochemical Society* 167, no. 12 (2020): 126504. https://doi.org/10.1149/1945-7111/abae91.

Zhang, Yang, Meiqin Zhang, Qianhui Wei, Yongjie Gao, Lijuan Guo, Khalid A. Al-Ghanim, Shahid Mahboob, and Xueji Zhang. "An easily fabricated electrochemical sensor based on a graphene-modified glassy carbon electrode

for determination of octopamine and tyramine." *Sensors* 16, no. 4 (2016): 535. https://doi.org/10.3390/s16040535.

VITA

Duygu BÜYÜKTAŞ

Education:

2015-2022 Ph.D., Department of Food Engineering, Faculty of Engineering, Izmir Institute of Technology, Izmir, Turkey

2010-2013 M.Sc., Department of Food Engineering, Faculty of Engineering, Izmir Institute of Technology, Izmir, Turkey

2004-2008 B.Sc., Department of Food Engineering, Faculty of Engineering, Ege University, Izmir, Turkey

Grants:

Tübitak 2214-A- International Research Fellowship Programme for Ph.D. Students
Council of Higher Education 100/2000 Ph.D. Scholarship

Publications:

Büyüktaş, Duygu, Masoud Ghaani, Cesare Rovera, Richard T. Olsson, Figen Korel, and Stefano Farris. "Development of a nano-modified glassy carbon electrode for the determination of 2, 6-diaminotoluene (TDA)." *Food Packaging and Shelf Life* 29 (2021): 100714.

Çavdaroğlu, Elif, **Duygu Büyüktaş**, Stefano Farris, and Ahmet Yemenicioğlu. "Novel edible films of pectins extracted from low-grade fruits and stalk wastes of sun-dried figs: Effects of pectin composition and molecular properties on film characteristics." *Food Hydrocolloids* 135 (2023): 108136.

Ghaani, Masoud, **Duygu Büyüktaş**, Daniele Carullo, and Stefano Farris. "Development of a New Electrochemical Sensor Based on Molecularly Imprinted Biopolymer for Determination of 4, 4′-Methylene Diphenyl Diamine." *Sensors* 23, no. 1 (2023): 46.